Transformer Winding Losses with Round Conductors and Foil Windings for Duty-Cycle Regulated Square Waveform Followed by Winding Design and Comparison for Sinusoidal Excitation

A THESIS
SUBMITTED TO THE FACULTY OF THE GRADUATE SCHOOL
OF THE UNIVERSITY OF MINNESOTA
BY

Kartik Iyer

IN PARTIAL FULFILLMENT OF THE REQUIREMENTS
FOR THE DEGREE OF
MASTER OF SCIENCE

Ned Mohan

December, 2013

Acknowledgements

First and foremost, I would like to thank my adviser, Prof. Ned Mohan for bestowing upon me this opportunity to work on this project. I would also like to extend my heartfelt gratitude to Prof. William P. Robbins for all those technical discussions that I had with him in the course of this project. I am really grateful to both Prof Mohan and Prof Robbins for the effort they took in reviewing my technical papers. I would also like to thank Dr. Oriol Valls who agreed to be in my committee for the thesis defense.

I want to express my gratitude to Eric Severson for his help and guidance in the first semester. I want to immensely thank Dr. Kaushik Basu for all the technical ideas and fruitful discussions. I am also very grateful to my friends, Ashish Sahoo, Srikant Gandikota and Srivatsal Sharma who have been good friends since we met in Minnesota. Also, lastly I thank all the other members in the PERL group.

I cannot miss out thanking my parents for their love and guidance. I want to especially thank my elder brother without whose support and advice nothing would have materialized.

Thank you very much and I love you all.

Dedication

To those who held me up over the years

Abstract

High frequency transformers are used extensively in Switch mode power supplies (SMPS). The transformer size reduces with an increase in frequency leading to a compact design. With the advent of SiC switches the SMPS can be operated at much higher frequencies. But with the increase in frequency, the losses in transformer increase. This poses a threat in the design of high density magnetic components. In order to design the magnetic components with smallest possible volume the estimation of the losses should be accurate. The losses in a transformer occur in the core as well as in the winding.

Simplified expressions for winding loss computation for duty cycle modulated current waveform for different conductors like foil and round is derived in this thesis. The thesis shows that the Fourier series method for the loss computation requires the consideration of a large number of harmonics leading to considerable computational difficulty in the determination of optimal thickness. A closed form approximate expression for power loss is presented that obviates any need for a large series summation resulting in a relatively simple computation of optimal thickness. In case of the solid round wire windings there is no optimal diameter for which the losses are minimum. The losses decrease with increasing diameter and there is a range of normalized diameters that should be avoided. A closed form approximate expression for a particular range of diameters of round wire depending on the current and frequency for power loss is presented that obviates any need for a large series summation.

The thesis also demonstrates a winding design procedure for minimizing the power losses using foils and solid round wires under sinusoidal excitation. In this thesis the range from which the thickness of the layers can be chosen to obtain the minimum power loss is derived. This thickness range is a function of the number of layers and does not include the "optimum" based on the previous literature. Using this design procedure, it is shown that interleaving is not necessary in foil -wound transformers to obtain the minimum loss. The analytical results are verified by designing six different winding configurations for the same specifications using 2-D Ansys Maxwell finite element design package.

Contents

List of Tables

List of Figures

Chapter 1

Introduction

Magnetic components like transformers are an integral part of Switch mode power supplies (SMPS). High frequency transformers determine about 25 % overall volume and more than 30 % of the overall weight of SMPS [1]. Hence, in order to reduce the footprint of SMPS the reduction in transformer volume is imperative. An increase in frequency allows for the volume reduction of transformers but at the cost of increased losses [2]. The losses occur in the core and in the windings of the transformer. The transformer is designed to be operated at low flux densities to avoid core saturation. Even at high frequency, due to the low flux density the core losses are less. The winding losses in the transformer depend on the number of turns and the winding dimensions. But at high frequencies due to eddy currents the effective conduction area reduces, which increases the losses. The increase in losses due to skin and proximity effects depend on the frequency and the winding type. Foil, solid-round wire, litz wires are the different conductors used in transformer winding [3]. The winding type applicable for a particular application depends primarily on the thermal requirement. A proper estimation of the winding losses is crucial for the design of high power density transformer. Even with a reasonable estimate of winding losses the ultimate goal is to design the transformer windings in a manner that increases the power density. For the design of low/medium power high frequency transformers, area product is the most common method for core selection. With solid-round, foil and litz wires being the different winding types, a lot of different winding design schemes are available, which might fit the given window specifications. A comparison of the different winding types is hence, inevitable so that

the designers have a fair idea of the winding type to be used for a given specification.

The eddy current effects on effective resistance of coils is shown in [4, 5]. But this effect on the transformer winding was first studied by [6]. In [6] winding losses are computed by considering a 1-D model of a transformer with foil windings. The 1-D model of the transformer does not take into account the effect of 2-D fields and hence can result in errors [7]. A lot of work has been done in literature to incorporate the 2-D effects [8], [9], [10], [11], [12]. Methods like resistance matrices have been developed to incorporate 2-D fields for gapped inductors and transformers [9]. Semi-empirical expressions are developed in [13]. However, the expressions derived in literature incorporating the 2-D effects are based on case studies, hence cannot be applied to other designs [10]. A detailed overview of the designs for which Dowell's 1-D method will work is provided in [14]. Improvements have been made in the Dowell's expression to include the layer porosity factor [15, 16]. The layer porosity factor does not have a theoretical base but is to be considered as an empirical correcting factor to model the increase in effective conducting section due to 2-D fields is shown in [17]. The winding loss analysis was extended to solid-round conductor by approximating the round conductors as foils [6, 18, 19]. But [20] showed that an orthogonality existed between skin and proximity effects which resulted in a more generalized analytical approach for loss computation of solid round conductors. The method was further improved in [21]. At high frequencies both [6] and [20] methods resulted in substantial errors of 60 % in eddy current loss computation for round conductors [22]. Analytical expressions using a look up table to compute the winding losses more accurately for round conductors were developed in [23]. But [23], also showed that if the layer porosity factor is high, as shown in [24] and [25], Dowell's 1-D expression with some modifications can be used to compute the losses with reasonable accuracy. In [26] the Dowell's 1-D expression for round conductors was modified further. The modified winding loss expression for solid round wire was used in [3] to compute losses for a solid-round wire inductor for sinusoidal excitation.

Switching circuits in power electronics lead to non-sinusoidal current waveforms through transformer windings [27], [28]. The losses in the transformer windings in case of non-sinusoidal currents will be more because of harmonics. In [29], for a non-sinusoidal waveform, the winding loss at each harmonic frequency is evaluated and then summed

up to give the total winding losses. In [29] winding losses are calculated for a unipolar rectangular waveform as encountered in forward converter topology. In [30] eddy current losses are calculated in rectifier transformers by approximating the functions given in [6]. The idea in [30] was developed in [31] to compute the optimal thickness for various non-sinusoidal currents. In [31]the losses for the solid-round wire were computed by approximating them as foil winding with modifications shown in [23]. The given formula in [31] to determine the optimal thickness was used in [32] to compare the single layer and multi-layer windings. The optimal thickness formula given in [31] and [32], is not very accurate for 1-3 layers. Also, as the formula depends on differentiation of the current waveform, it cannot be used in case of duty cycle regulated square waveforms with negligible rise times. Typically, switching times of high power IGBTs are in order of hundreds of nano-seconds and switching frequency is in tens of kilohertz. In [33], the winding losses are computed for non-sinusoidal currents in solid-round conductors. For a duty-cycle regulated square waveform the winding losses depend on a large number of harmonics as shown in [34]. In [34] an approximate expression to compute the power loss independent of harmonics for foil windings was shown.

The windings in magnetic components may be foil conductors [35], [36] or litz wires [37], [38]. The optimum thickness of foil conductors obtained by the 1-D analysis, as a function of number of layers, were used to design the foil conductors [39]. However, the designs at optimal thicknesses resulted in ac losses more than the dc losses. Losses can be reduced if the winding can be designed such that the ac losses match the dc losses. A comparison between foil and solid-round conductors for a particular design was shown in [40] which showed that the foil conductors are less lossy than round conductors but still are more than dc losses. In [1] it was shown that the foil conductors should be extremely thin to have low losses. This led to the use of extremely thin strips of conductor at high frequencies known as litz wires, which have ac losses same as the dc losses. The optimal design and the cost analysis of litz wires were done in [41] and [42] respectively. But the litz wires are expensive and the window utilization factor is low. The choice between foil and litz wire is difficult and it depends on various design trade offs as shown in [43]. In literature, the comparison between different winding types are more for specific cases than a generalized comparison [40], [43].

1.1 Contribution of the thesis

The winding loss for a duty-cycle regulated square waveform, was done in [29], [31]. But the number of harmonics considered is fairly limited. In this thesis, it is shown that for large number of layers, large number of harmonics have to be considered to accurately predict AC power loss. This also implies difficulty in the computation of optimal winding thickness by considering AC power loss as a sum of large number of harmonics. An approximate formula for AC power loss is derived, that does not involve any series summation with large number of terms and leads to comparatively easy determination of the optimal winding thickness for a given number of layers and duty cycle D.

The winding loss for duty-cycle regulated square waveform in a transformer with solid round-wire windings is also computed. It is shown that there is no optimal diameter of the conductor for which the AC power loss is minimum. The AC power loss keeps reducing as the diameter increases. A generalized relation between current and normalized diameter (independent of frequency) is also shown. It is demonstrated that there is a particular range of normalized diameter that should be avoided. It also shows approximate power loss expressions for other ranges of normalized diameter. The approximate expression is verified using numerical computation. The analytical results are verified using 2-D FEM results in two ways. A generalized case, independent of frequency, in which the core dimensions vary to fit the specified number of turns in the window. Also, two specific cases, in which the transformer core is chosen using area product method and the losses are validated using 2-D FEM.

The foil winding design procedure is analyzed and it is shown that it is possible to design foil so that the ac to dc resistance is close to 1 thereby giving an alternative to the expensive litz wires. It is also shown in the thesis that if designed effectively the interleaving to minimize winding losses can be avoided. The conventional and the proposed way of winding design using foil conductors is shown followed by a step-by-step winding design procedure for foil and solid round conductor. Six different winding configuration for the same specifications is considered and power loss for each is computed and validated using 2-D FEM.

- Chapter 1 gives an introduction.

- Chapter 2 briefly presents the reasons for increase in winding losses at high frequency and the need to minimize the losses.
- In Chapter 3 the normalized power loss expression for duty-cycle modulated current waveform for foil windings is presented.
- Chapter 4 presents the normalized and simplified power loss expression for solid round wire windings.
- Chapter 5 demonstrates a design procedure and comparison between foil and solid-round conductors.
- Chapter 6 presents the conclusion and the future work.

Chapter 2

Skin and Proximity Effects in Transformer Windings

With the advancement in the semiconductor switches, there in an increase in trend to operate switch mode power converters at high frequencies. The transformer size reduces with increase in frequency, enabling a compact design. However, the losses in the transformer increase with the frequency. The factors primarily responsible for the increase in the losses are

- Skin Effect.
- Proximity Effect.

The cause and the impact of these effects on the transformer winding losses is explained in this chapter.

2.1 Skin Effect

The transformer windings have a specific dc resistance which depends on the winding dimensions, the number of turns and the material. This dc resistance induces the copper losses. The power loss in a single isolated winding excited by a dc current I, is,

$$P_{dc} = I^2 R_{dc} \tag{2.1}$$

where,

$$R_{dc} = \frac{\rho(MLT)}{da} \tag{2.2}$$

ρ is the resistivity of the winding material. For copper (which is normally used as a winding material $\rho = 1.68 \times 10^{-8}\Omega m$ at $20\,^{\circ}$C). MLT is the Mean Length of Turns, d is the thickness of the foil conductor and a is the width of the foil conductor.

The alternating currents induce a magnetic flux, ϕ, which follow circular paths around the current. According to Lenz's law, these flux lines induce eddy currents which flow in a manner so as to oppose induced magnetic flux, ϕ. These induced eddy currents flow in the opposite direction to the applied ac current in the interior of the conductor and hence, shields the interior of the conductor from the applied current. The current density, $J_{rms} = \frac{I_{rms}}{A_w}$, where A_w is the area of the foil conductor. Because of the eddy currents, the current density, is maximum at the surface of the conductor and decreases exponentially towards the interior of the conductor. The thickness at which the current density reduces to $1/e$ of the current density at the surface of the conductor is called the skin depth. (2.3) is used to compute the skin depth.

$$\delta = \frac{1}{\sqrt{\pi f \mu \sigma}} \tag{2.3}$$

where, $\mu = 4\pi \times 10^{-7} H/m$, $\sigma = 5.8 \times 10^{-7}\ S/m$ for copper and f, is the frequency. So, the effective conductor area through which the applied current flows, reduces and hence, as can be seen from (2.2), the resistance increases. This increase in the ac resistance compared to the dc resistance increases the losses in the transformer termed as skin effect losses.

It can be seen from (2.3) that as the frequency increases the skin depth reduces. In line frequency transformers, as the frequency is 50/60 Hz the skin depth is high as compared to the skin depth at high frequencies and if the winding thickness is less than the skin depth then there will be no increase in losses due to skin effect. In high frequency transformers, as the frequency is high the skin depth is low which increases the possibility of losses due to skin effect.

The current density distribution, and the flux density distribution on one isolated conductor for thicknesses less than and more than skin depth is shown using 2-D Finite Element Modeling (FEM), ANSYS MAXWELL 16.0.

Fig. 2.1, shows an isolated foil winding of thickness $d = 0.1mm$. This winding is excited by a unit rms sinusoidal current at $f = 1000Hz$. The skin depth at $f = 1000Hz$ is $\delta = 2.089mm$ using (2.3). As the conductor thickness is less than the skin depth hence the J distribution is continuous as shown in Fig. 2.1. The effective area is $A_w = a \times d$. Hence, the ac resistance will be the same as the dc resistance. If the conductor thickness is much more than the skin depth ($d = 8.356mm > \delta = 2.089mm$) then as shown in Fig. 2.2 the currents will primarily flow only through the edges of the winding, leading to discontinuous J distribution, which will reduce the effective area and hence increase the losses. The effective area is $A_w = 2 \times a \times \delta$.

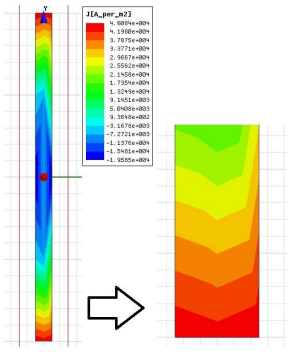

Figure 2.1: Current density distribution in an isolated foil conductor of thickness less than skin depth

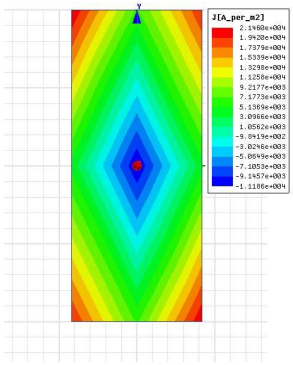

Figure 2.2: Current density distribution in an isolated foil conductor of thickness more than skin depth

The power loss in a single isolated winding with thickness more than skin depth

excited by an ac current I, is,

$$P_{ac} = I^2 R_{ac} \tag{2.4}$$

where,

$$R_{ac} = \frac{\rho(MLT)}{2\delta a} \tag{2.5}$$

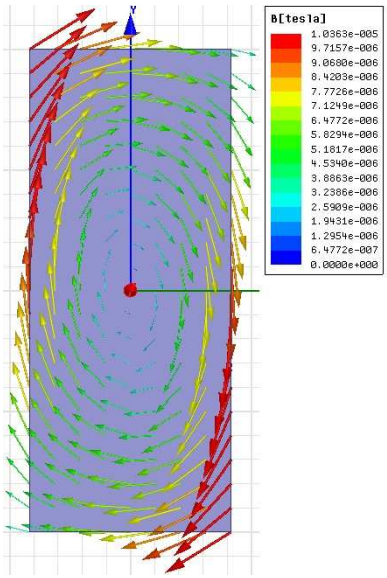

Figure 2.3: B-field distribution in an isolated foil conductor

Fig. 2.3 shows the magnetic field distribution in a single layer isolated foil winding.

2.2 Proximity Effects

The alternating current flowing in a conductor generates a magnetic field. If the adjacent conductors are in a close proximity to this conductor, then the magnetic field will induce eddy currents in that conductor. The eddy current causes a change in the current density distribution in both the conductors whether or not there is any current in that adjacent conductor. In this section the effect of conductors present in a proximity, on current density distribution, J and magnetic field, B of the conductor is shown. Fig. 2.4, shows a single layer each of both primary and secondary foil winding of thickness $d = 8.356mm$. The primary winding is excited by a unit rms sinusoidal current at

$f = 1000Hz$ while the secondary is open and no current flows through it. The skin depth at $f = 1000Hz$ is $\delta = 2.089mm$.As the conductor thickness is more than the skin depth ($d = 8.356mm > \delta = 2.089mm$) then as shown in Fig. 2.4 the currents will primarily flow only through the edges of the winding, leading to discontinuous J distribution, which will reduce the effective area and hence increase the losses. It is to be noted that the current density distribution in Fig. 2.4 is different from that as shown in Fig. 2.2 because of proximity effects. As a result of this the effective area is different from the case of single layer isolated foil winding. The effective area is $A_w = a \times \delta$. Fig. 2.5 shows the magnetic field distribution in a single layer each of primary and secondary foil winding. As compared to Fig. 2.3, the magnetic field distribution is much different in Fig. 2.5 dure to proximity effects.

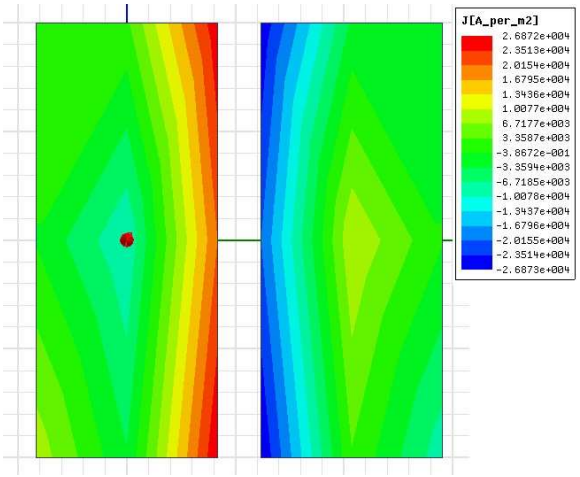

Figure 2.4: Current density distribution in 1-layer each of both primary and secondary foil winding.

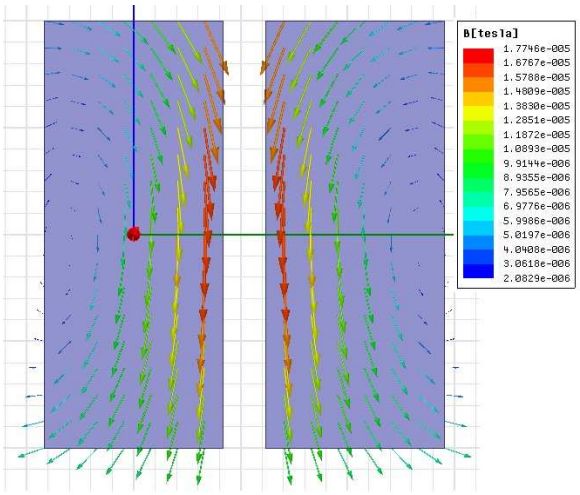

Figure 2.5: B-field distribution in 1-layer each of both primary and secondary foil winding

The power loss in a single layer winding each of primary and secondary of a transformer with thickness more than skin depth excited by an ac current I, is,

$$P_{ac} = I^2 R_{ac} \tag{2.6}$$

where,

$$R_{ac} = \frac{\rho(MLT)}{\delta a} \tag{2.7}$$

Fig. 2.7, shows three layers each of both primary and secondary foil winding of thickness $d = 8.356mm$. In this case both primary and the secondary winding are excited by a unit rms sinusoidal current at $f = 1000Hz$. The skin depth at $f = 1000Hz$ is $\delta = 2.089mm$.As the conductor thickness is more than the skin depth ($d = 8.356mm > \delta = 2.089mm$) then as shown in Fig. 2.7 the currents will primarily flow only through the edges of the winding, leading to discontinuous J distribution, which will reduce the effective area and hence increase the losses. The effective area is $A_w = a \times \delta$. Fig. 2.5 shows the magnetic field distribution in three layers of foil winding. It can be seen from the B-field distribution that along with skin effect losses there are also losses due to proximity effect. If more and more layers, with the same thickness are stacked together, the losses due to proximity effect will keep increasing.

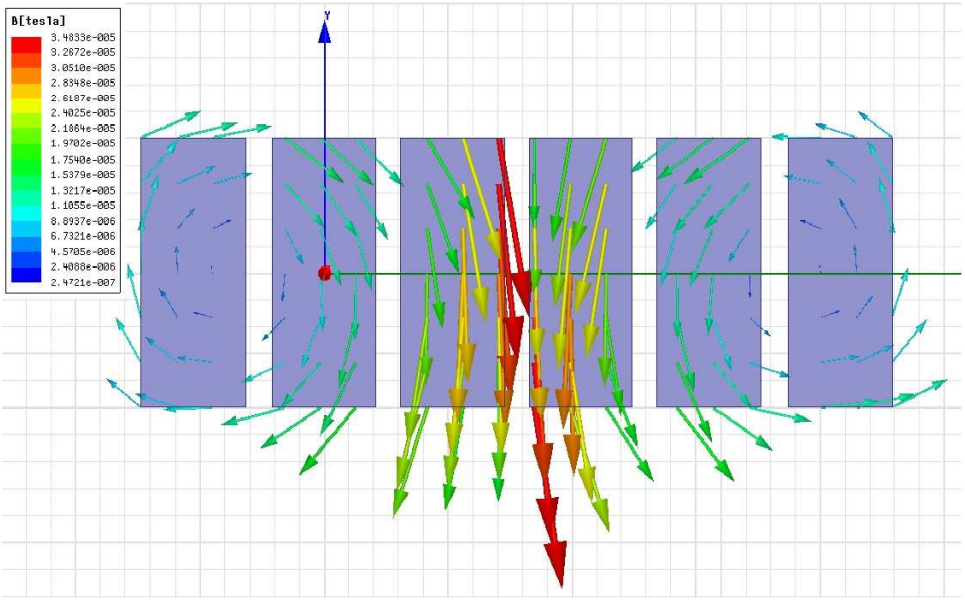

Figure 2.6: B-field distribution in three layers of both primary and secondary foil winding

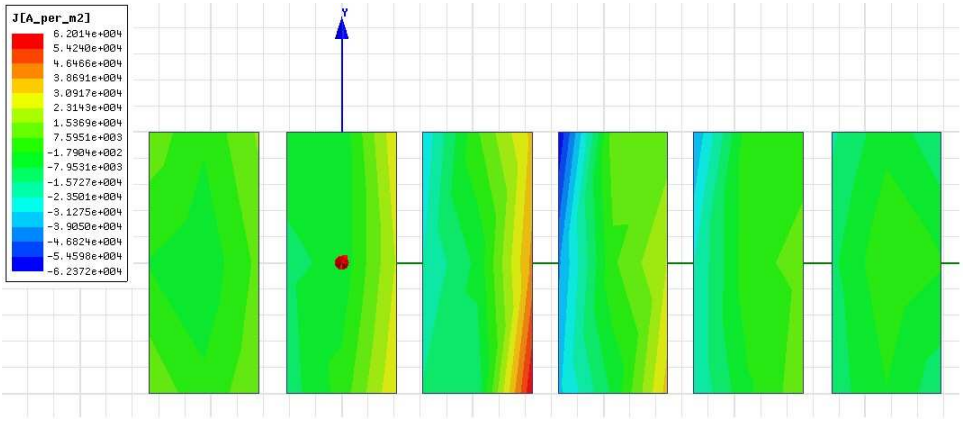

Figure 2.7: Current density distribution in three layers of both primary and secondary foil winding.

The AC power loss expression considering both skin and proximity effects is explained in the next section.

2.3 AC Power Loss Expression

The AC power loss expression computed for p layers as shown in [6] in rectangular coordinate system is derived in the APPENDIX. The power loss formula, hence computed is shown below,

$$P = 2I^2 \frac{\rho(MLT)N^2}{h\delta p\eta} \left[\frac{\sinh(2\Delta) + \sin(2\Delta)}{\cosh(2\Delta) - \cos(2\Delta)} + \frac{2}{3}(p^2 - 1)\frac{\sinh(\Delta) - \sin(\Delta)}{\cosh(\Delta) + \cos(\Delta)} \right] \tag{2.8}$$

where, I is the rms current amplitude, ρ is the resistivity of copper, N is the total number of turns in one winding, p is the total number of layers, MLT is the Mean Length of Turns and $\Delta = \frac{d}{\delta}$, where d is the thickness of the foil conductor and δ is the skin depth.

Fig. 2.8 shows a plot of ac power loss for different layers for a range of Δ, where height of the window h is assumed to be a constant and much much greater than d . It can be seen that for all layers after a particular Δ the power loss becomes almost constant. This is because when thickness $d >> \delta$, then the current only flows in the thin strip of δ, and not over the whole conductor thickness and as the width of the conductor is assumed to be much larger than the thickness and assumed to be a constant the power loss becomes almost constant.

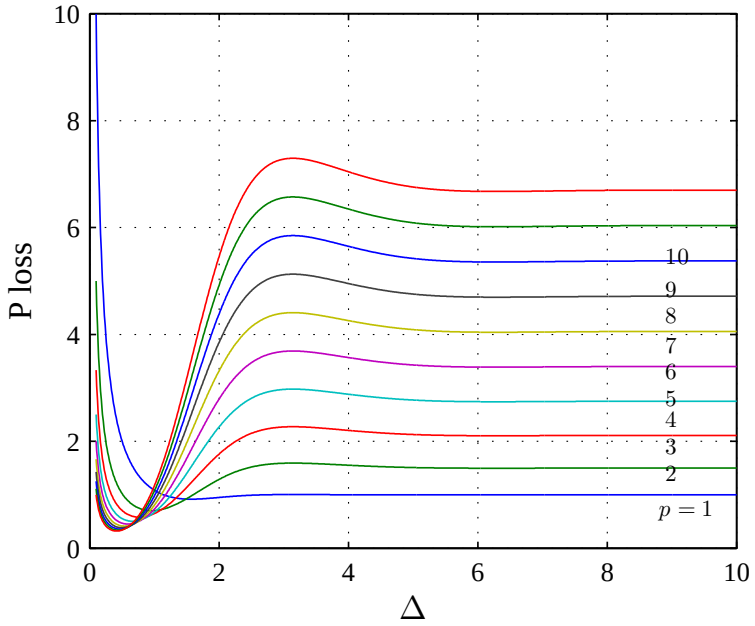

Figure 2.8: Plot of Power loss with Δ for different layers, p

Fig. 2.9 shows the plot for smaller values of δ. The width of the conductor is considered to be constant. For $\Delta < 1$, there will be no skin effect losses as the thickness of the conductor is less than the skin depth. The dc losses will be high as the thickness is small. As Δ keeps on increasing as shown in Fig. 2.9 that for each layer there is a δ_{opt}, when the losses are minimum.

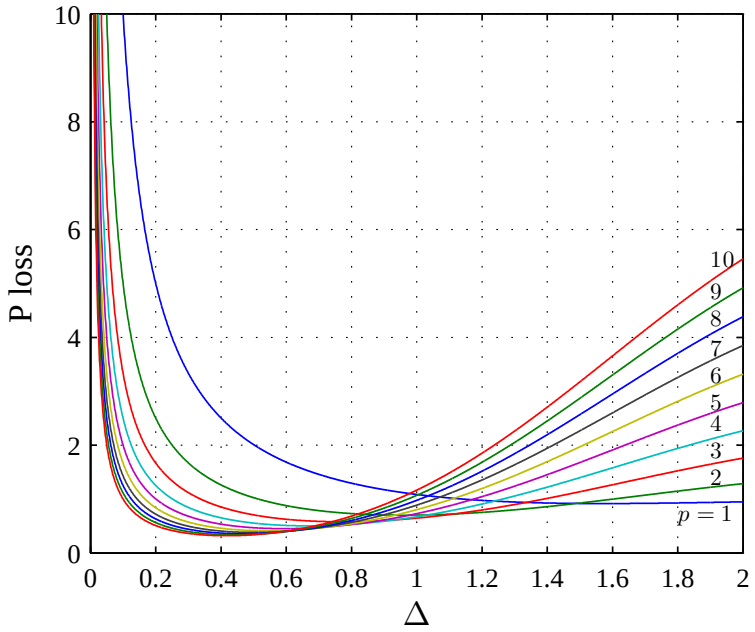

Figure 2.9: Plot of Power loss with Δ ranging from 0 to 2 for different layers, p

The following chapters will give a detailed description on the ac winding losses for foil conductors and solid round conductors for a duty cycle regulated square waveform.

Chapter 3

Transformer Winding Losses with Foil Conductors for Duty-Cycle Regulated Square Waves

In the last chapter the transformer winding losses for a sinusoidal current excitation was presented. In [29], for a non-sinusoidal waveform, the winding loss at each harmonic frequency is evaluated and then summed up to give the total winding losses. In this chapter it is shown that the losses for a duty-cycle regulated square waveform depends on a large number of harmonics, hence making the computation difficult.

3.1 Variation of P with harmonics

A bipolar duty cycle modulated square current waveform is considered as shown in Fig. 3.1. This current can be represented by the following Fourier series:

$$i(t) = I_0 + \sum_{k=1}^{\infty} \sqrt{2} I_k \sin(k\omega t) \tag{3.1}$$

where,

$$I_k = \frac{2\sqrt{2} I \sin(\frac{k\pi D}{2})}{k\pi} \tag{3.2}$$

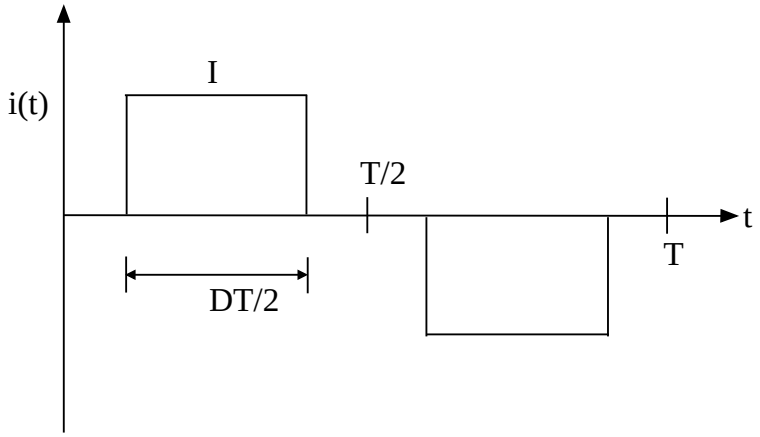

Figure 3.1: Duty-cycle regulated current waveform

and as the waveform is symmetric,

$$I_0 = 0 \tag{3.3}$$

The AC power loss expression can be written as [6],

$$\begin{aligned} P &= \sum_{k=1}^{\infty} \frac{8I^2 \sin^2(\frac{k\pi D}{2})}{k^{\frac{3}{2}}\pi^2} \frac{\rho(MLT)N^2}{h\delta p\eta} \left[\frac{\sinh(2\sqrt{k}\Delta) + \sin(2\sqrt{k}\Delta)}{\cosh(2\sqrt{k}\Delta) - \cos(2\sqrt{k}\Delta)} \right. \\ &\quad \left. + \frac{2}{3}(p^2-1) \frac{\sinh(\sqrt{k}\Delta) - \sin(\sqrt{k}\Delta)}{\cosh(\sqrt{k}\Delta) + \cos(\sqrt{k}\Delta)} \right] \end{aligned} \tag{3.4}$$

Here, it is assumed that,

$$P_{base} = \frac{8I^2}{\pi^2} R_{dc}|_{d=\delta} \tag{3.5}$$

where,

$$R_{dc}|_{d=\delta} = \frac{N^2\rho(MLT)}{h\delta p\eta} \tag{3.6}$$

The dc resistance of a single layer of a transformer containing multiple turns at a thickness equal to the skin depth of the conductor as shown in Fig. 3.2 is

$$R_{dc}|_{d=\delta} = \frac{N_l\rho(MLT)}{a\delta} \tag{3.7}$$

For a transformer, containing p layers, the $R_{dc}|_{d=\delta}$ takes the form,

$$R_{dc}|_{d=\delta} = \frac{N_l\rho(MLT)p}{a\delta} \tag{3.8}$$

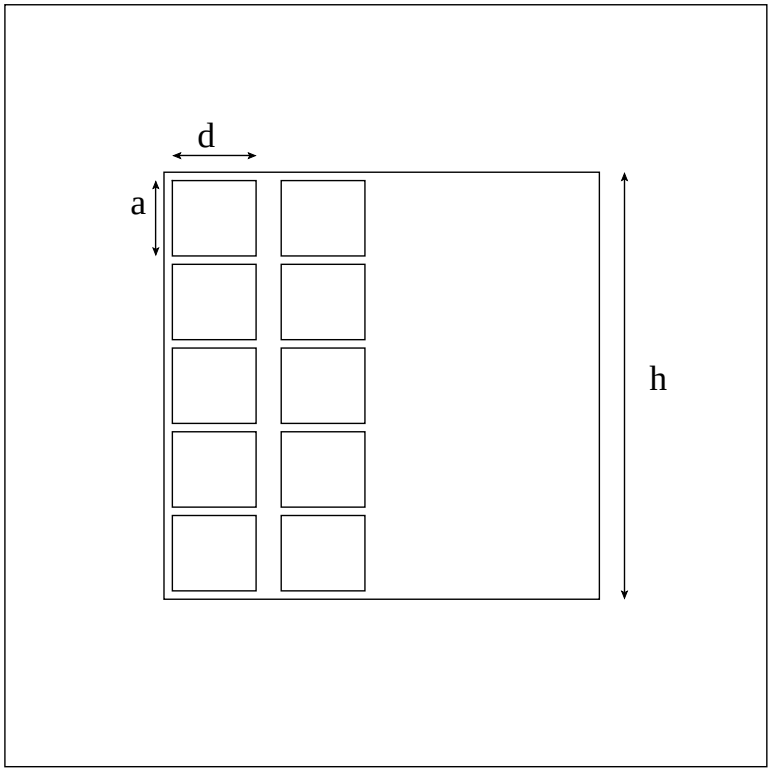

Figure 3.2: Multi-turn Multi-layer foil winding of a transformer.

Substituting a as $\eta h/N_l$ and $N_l p$ as N,

$$R_{dc}|_{d=\delta} = \frac{N^2 \rho (MLT)}{h \delta p \eta} \tag{3.9}$$

Hence,

$$\begin{aligned} \frac{P}{P_{base}} &= P_{pu} = \sum_{k=1}^{\infty} \frac{\sin^2(\frac{k\pi D}{2})}{k^{\frac{3}{2}}} \times \left[\frac{\sinh(2\sqrt{k}\Delta) + \sin(2\sqrt{k}\Delta)}{\cosh(2\sqrt{k}\Delta) - \cos(2\sqrt{k}\Delta)} \right. \\ &\left. + \frac{2}{3}(p^2 - 1) \frac{\sinh(\sqrt{k}\Delta) - \sin(\sqrt{k}\Delta)}{\cosh(\sqrt{k}\Delta) + \cos(\sqrt{k}\Delta)} \right] \end{aligned} \tag{3.10}$$

As seen from (3.10), each harmonic component of P_{pu} falls as a function of $k^{\frac{3}{2}}$. For a duty cycle modulated square current waveform, large number of harmonics have to be considered, as $k^{\frac{3}{2}}$ is a slowly decaying function. Fig. 3.3, shows a plot of

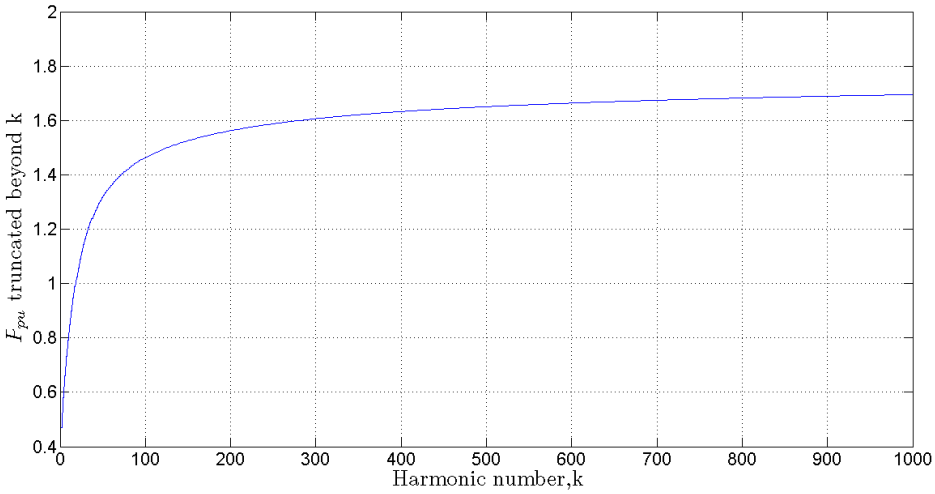

Figure 3.3: Plot of approximate P_{pu} beyond k at $\Delta = 0.5$, for p=5, D=1 with k.

P_{pu} approximated by truncating (3.10) for a specified number of harmonics at a given $\Delta = 0.5$, for 5 layers and $D = 1$. Ideally, infinite number of harmonics have to be considered but in practice only a finite number of harmonics can be used to compute P_{pu} approximately. But Fig. 3.3, shows that large number of harmonics have to be considered to avoid significant errors. Hence, it is computationally difficult to calculate the power loss using Fourier analysis method.

By using trigonometric identities (3.10) can be written as,

$$P_{pu} = \sum_{k=1}^{\infty} \frac{\sin^2(\frac{k\pi D}{2})}{k^{\frac{3}{2}} p} \left[\frac{G_1}{2} + \frac{(4p^2-1)}{6} G_2 \right] \tag{3.11}$$

where G_1 and G_2 are,

$$G_1 = \frac{\sinh(\sqrt{k}\Delta) + \sin(\sqrt{k}\Delta)}{\cosh(\sqrt{k}\Delta) - \cos(\sqrt{k}\Delta)} \tag{3.12}$$

$$G_2 = \frac{\sinh(\sqrt{k}\Delta) - \sin(\sqrt{k}\Delta)}{\cosh(\sqrt{k}\Delta) + \cos(\sqrt{k}\Delta)} \tag{3.13}$$

The asymptotic values of both the functions in (3.12) and (3.13) approach 1 for $\sqrt{k}\Delta > 2.5$, as given in [31]. Hence, for each Δ there is a particular harmonic number beyond which the product $\sqrt{k}\Delta > 2.5$ and the harmonic component of the power loss becomes

independent of Δ. For $\sqrt{k}\Delta > 2.5$, both (3.12) and (3.13) become 1 and P_k, the k^{th} component of P_{pu} is,

$$P_k = \frac{\sin^2(\frac{k\pi D}{2})}{k^{\frac{3}{2}}}\left(\frac{2p^2+1}{3}\right) \tag{3.14}$$

For $\sqrt{k}\Delta < 2.5$ as shown in [31], P_k can be written as,

$$P_k = \frac{\sin^2(\frac{k\pi D}{2})}{k^{\frac{3}{2}}}\left[\frac{1}{\sqrt{k}\Delta} + \left(\frac{5p^2-1}{45}\right)k^{3/2}\Delta^3\right] \tag{3.15}$$

Now, (3.10) which is an infinite series sum depending on Δ, can be split into a finite sum that depends on Δ and an infinite sum independent of Δ.

$$\begin{aligned} P_{pu} &= \left[\frac{1}{\Delta}\sum_{k=1}^{N_\Delta}\frac{\sin^2(\frac{k\pi D}{2})}{k^2} + \left(\frac{5p^2-1}{45}\right)\Delta^3\sum_{k=1}^{N_\Delta}\sin^2\left(\frac{k\pi D}{2}\right)\right. \\ &\quad \left. + \left(\frac{2p^2+1}{3}\right)\sum_{k=N_\Delta+1}^{\infty}\frac{\sin^2\left(\frac{k\pi D}{2}\right)}{k^{\frac{3}{2}}}\right] \end{aligned} \tag{3.16}$$

where, N_Δ is the harmonic number beyond which the harmonic components of P_{pu} does not depend on Δ. Now, the third term in (3.16) can be written as,

$$\sum_{k=N_\Delta+1}^{\infty}\frac{\sin^2(\frac{k\pi D}{2})}{k^{\frac{3}{2}}} = \sum_{k=1}^{\infty}\frac{\sin^2(\frac{k\pi D}{2})}{k^{\frac{3}{2}}} - \sum_{k=1}^{N_\Delta}\frac{\sin^2(\frac{k\pi D}{2})}{k^{\frac{3}{2}}} \tag{3.17}$$

The three finite summations can be represented as a function of N_Δ, for a given duty ratio D, by curve fitting formula. The curve fitting formula is of the form $aN_\Delta^b + c$. By using the relation, $N_\Delta = (\frac{2.5}{\Delta})^2$ the power loss P_{pu} can be represented in terms of Δ. Hence, (3.16) takes the form,

$$\begin{aligned} P_{pu} &= \frac{1}{\Delta}\left[k_1\left(\frac{2.5}{\Delta}\right)^{k_2} + k_3\right] + \left(\frac{5p^2-1}{45}\right)\left(3.125\Delta + k_4\Delta^3\right) + \left(\frac{2p^2+1}{3}\right) \\ &\quad \times\left[k_5 - \left(k_6\left(\frac{2.5}{\Delta}\right)^{2k_7} + k_8\right)\right] \end{aligned} \tag{3.18}$$

The value of k_5 is an infinite series sum which is known. The constants k_1 to k_8 in (3.18) are functions of duty cycle D. These constants are given in Table 3.1 for different

values of D. For a given current waveform (with a specific value of D), (3.18) can be used to estimate the power loss for a given thickness Δ and number of layers, p.

Table 3.1: Value of constants for specific duty ratios

Coefficients	$D = 0.25$	$D = 0.5$	$D = 0.75$	$D = 1$
k_1	-0.4153	-0.413	-0.3165	-0.4505
k_2	-0.9201	-0.9677	-0.821	-0.979
k_3	0.5402	0.9252	1.158	1.234
k_4	0.2426	0.25	0.2512	0.2515
k_5	1.0785	1.4413	1.6293	1.6886
k_6	-0.9608	-0.9089	-0.8393	-0.8145
k_7	-0.4904	-0.4706	-0.4325	-0.4175
k_8	1.079	1.445	1.642	1.705

3.2 Computation of Δ_{opt}

There have been several ways proposed to calculate Δ_{opt}, [31] [44]. In [31], Δ_{opt} is represented in terms of the rms of differentiated current waveform, which is a closed form formula but it cannot be used for duty cycle modulated square waveforms with negligible risetimes. In [31], the entire series was approximated by (3.15). This approximation is not particularly true for low number of layers.

To compute Δ_{opt} using (3.10), N_Δ should be known. For smaller layers the value of Δ_{opt} is close to 1, hence N_Δ is small. Therefore, for smaller layers, only few harmonics are required for computation of Δ_{opt}. Whereas, for larger number of layers the value of Δ_{opt} is much less than 1. Hence, N_Δ is very large. Therefore, in order to compute Δ_{opt} large number of harmonics have to be considered. In [44], Δ_{opt} is represented in terms of a ratio of two series summations but the harmonic number till which the summations are to be carried out is not mentioned.

Differentiation of (3.18) with respect to Δ, gives an implicit equation involving Δ_{opt},

(3.19)

$$\frac{-1}{\Delta_{opt}^2}\left[k_1\left(\frac{2.5}{\Delta_{opt}}\right)^{2k_2}(2k_2+1)+k_3\right]+\left(\frac{5p^2-1}{45}\right)\left(3.125+3k_4\Delta_{opt}^2\right)$$
$$+\left(\frac{2p^2+1}{3}\right)\left[k_6\left(\frac{2.5}{\Delta_{opt}}\right)^{2k_7}\left(\frac{2k_7}{\Delta_{opt}}\right)\right]=0 \tag{3.19}$$

Δ_{opt} can be obtained by solving, (3.19) numerically. Δ_{opt} can also be computed using MATLAB's optimization toolbox.

$$\Delta_{opt}=m_1p^{m_2}+m_3 \tag{3.20}$$

Table 3.2, gives coefficients of a curve fitting formula shown in (3.20), to compute Δ_{opt} for specific duty ratios, for 1-25 layers.

Table 3.2: Coefficients for computation of Δ_{opt}

Coefficients	$D=0.25$	$D=0.5$	$D=0.6$	$D=0.75$	$D=0.8$	$D=1$
m_1	1.134	1.394	1.402	1.518	1.529	1.553
m_2	-1.112	-1.061	-0.993	-1.026	-1.022	-1.016
m_3	0.01386	0.0107	-0.001025	0.005249	0.004716	0.003636

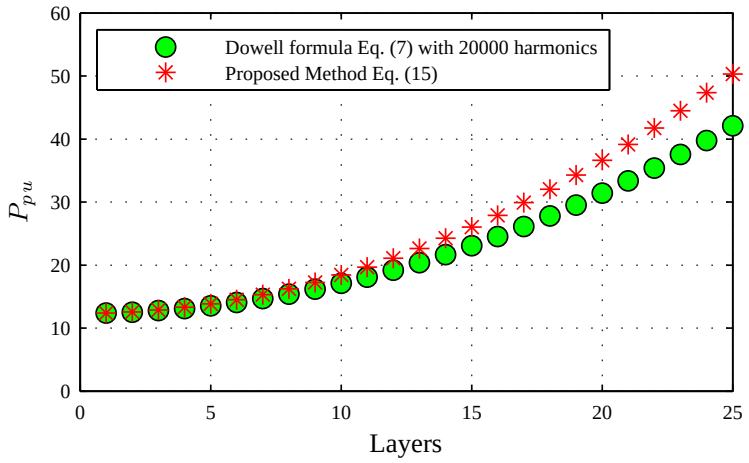

Figure 3.4: Comparison of different methods for computation of P_{pu}.

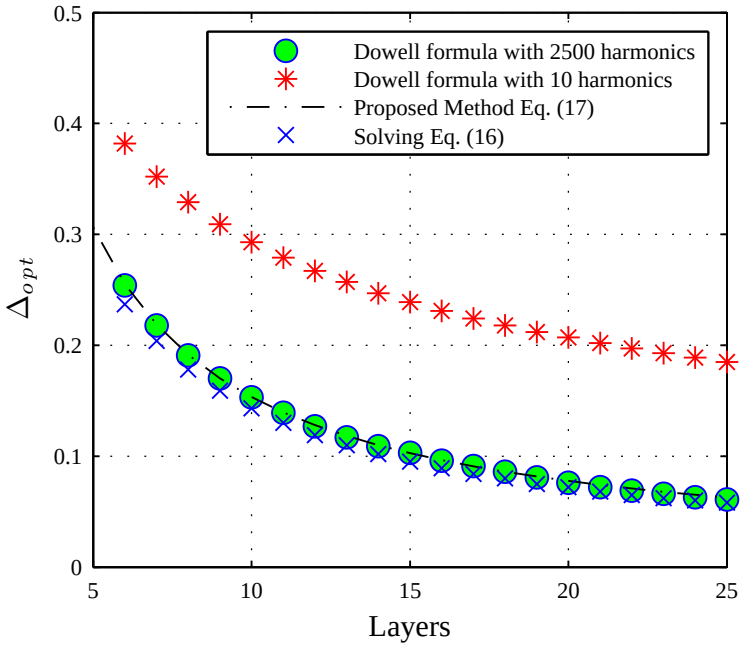

Figure 3.5: Comparison of different methods for computation of Δ_{opt}.

3.3 Validation of results

A duty cycle modulated square waveform of duty ratio $D = 1$ is considered. A MATLAB code is written to compute P_{pu} using (3.10) by considering 20000 harmonics for 1-25 layers at Δ=0.1. P_{pu} is also computed by solving (3.18) and Fig. 3.4 shows a comparison of both methods. Then Δ_{opt} is obtained by searching the minimum value of P_{pu}. Δ_{opt} is also found by solving (3.19) and by solving (3.20) and a comparison of all three methods is shown in Fig. 3.5. If (3.10) is used to compute Δ_{opt} graphically for $p = 2$, Δ_{opt} is 0.764, so only 11 harmonics are required to compute Δ_{opt}. But for $p = 8$, Δ_{opt} is 0.191, so 172 harmonics are required to compute Δ_{opt}. If only 10 harmonics are considered then for $p = 8$, Δ_{opt} is 0.329 leading to an error of 72%. On the other hand, if (3.19) is solved using MATLAB for $p = 8$, Δ_{opt} is 0.175, leading to an error of 8.4%. Finally if (3.20) is used then Δ_{opt} is 0.1893, leading to an error of 0.91%. This confirms the advantage and efficiency of the method proposed. Once Δ_{opt} is determined for a given layer p, optimal value of d can be found. Using (3.18) it is possible to obtain an estimate of power

loss for a given layer p at the optimal thickness. In the next chapter the estimation of winding loss will be extended for solid round conductors for a duty-cycle regulated square current excitation.

Chapter 4

Winding Losses in Round Conductors for Square Currents

In the last chapter the transformer winding losses for a duty-cycle regulated square waveform was presented. In [33] the winding losses for a non-sinusoidal waveform for solid-round conductor was presented. The number of harmonics that were considered were less. In this chapter it is shown that on considering large number of harmonics, the existance of valley diameter and hill diameter as shown in [3] is no longer present. The losses keep decreasing with the increasing diameter.

The ac to dc resistance ratio F_R for solid round-wire windings and sinusoidal current is [6], [3]

$$F_R = \Delta \left[\frac{\sinh(2\Delta) + \sin(2\Delta)}{\cosh(2\Delta) - \cos(2\Delta)} + \frac{2}{3}(p^2 - 1)\frac{\sinh(\Delta) - \sin(\Delta)}{\cosh(\Delta) + \cos(\Delta)} \right] \tag{4.1}$$

where Δ is,

$$\Delta = \left(\frac{\pi}{4}\right)^{0.75} \frac{d}{\delta}\sqrt{\eta} \tag{4.2}$$

The diameter of solid round-wire winding is d. δ is the skin depth at the fundamental frequency and η is d/l where, l is the distance between centers of adjacent round conductors as shown in Fig. 4.1. A bipolar duty-cycle regulated square current waveform is considered as shown in Fig. 3.1. This current can be represented by the following Fourier series:

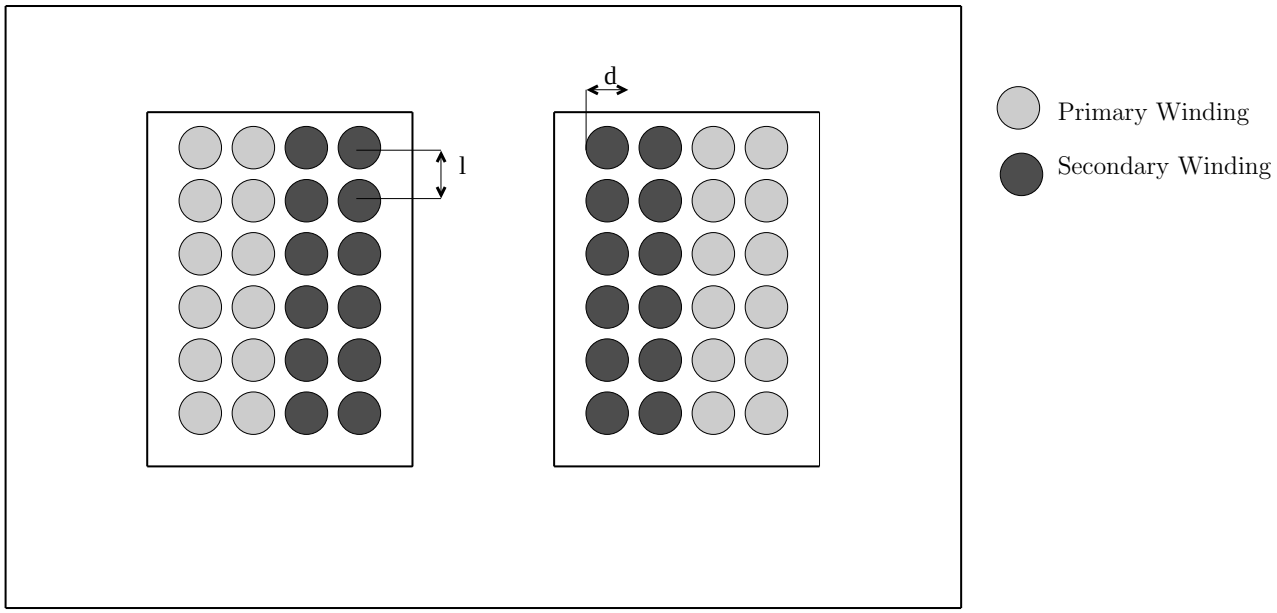

Figure 4.1: Solid-round wire winding of a transformer

$$i(t) = I_0 + \sum_{k=1}^{\infty} \sqrt{2} I_k \sin(k\omega t) \text{ where, } \quad I_k = \frac{2\sqrt{2} I \sin(\frac{k\pi D}{2})}{k\pi} \tag{4.3}$$

and as the waveform is symmetric, $I_0 = 0$. The power loss expression for solid round-wire conductors for one winding can be written as [6],

$$\begin{aligned} P \;=\; & \sum_{k=1}^{\infty} \frac{8I^2 \sin^2(\frac{k\pi D}{2})}{k^{\frac{3}{2}}\pi^2} \frac{\rho(MLT)N\eta}{\delta^2\Delta} \sqrt{\frac{\pi}{4}} \left[\frac{\sinh(2\sqrt{k}\Delta) + \sin(2\sqrt{k}\Delta)}{\cosh(2\sqrt{k}\Delta) - \cos(2\sqrt{k}\Delta)} \right. \\ & \left. + \frac{2}{3}(p^2 - 1) \frac{\sinh(\sqrt{k}\Delta) - \sin(\sqrt{k}\Delta)}{\cosh(\sqrt{k}\Delta) + \cos(\sqrt{k}\Delta)} \right] \end{aligned} \tag{4.4}$$

where, P is the AC power loss, D is the Duty ratio of square waveform, p is the number of layers, k is the harmonic number, ρ is the resistivity of copper, I is the peak value of square current, N_l is the number of turns per layer, N is the total number of turns ($= N_l p$) and MLT is the Mean Length of Turns.

The dc resistance of a transformer containing N multiple turns at a diameter equal to the skin depth of the conductor is given in (4.5). Now P_{base} given by (4.6) can be

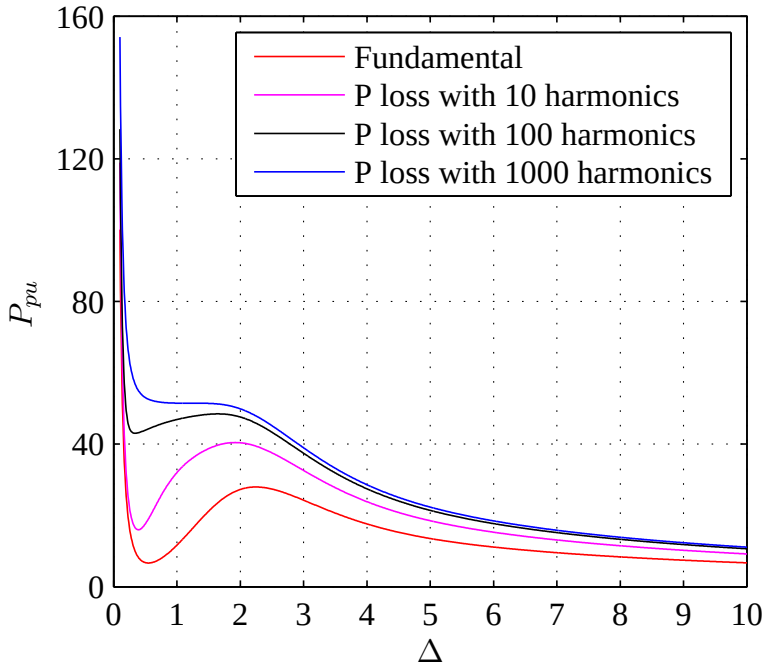

Figure 4.2: Plot of P_{pu} using (4.4) versus Δ for p=10 and D=1 for different numbers of harmonics

written in terms of $R_{dc}|_{d=\delta}$ as shown in (4.7).

$$R_{dc}|_{d=\delta} = \frac{N\rho(MLT)}{\frac{\pi}{4}\delta^2} \tag{4.5}$$

$$P_{base} = \frac{8I^2}{\pi^2}\frac{N\rho(MLT)\eta}{\delta^2}\sqrt{\frac{\pi}{4}} \tag{4.6}$$

$$P_{base} = \frac{I^2\eta R_{dc}|_{d=\delta}}{\sqrt{\pi}} \tag{4.7}$$

Using, (4.7), P can be written as,

$$\begin{aligned}\frac{P}{P_{base}} &= P_{pu} = \sum_{k=1}^{\infty}\frac{\sin^2(\frac{k\pi D}{2})}{\Delta k^{\frac{3}{2}}} \times \left[\frac{\sinh(2\sqrt{k}\Delta)+\sin(2\sqrt{k}\Delta)}{\cosh(2\sqrt{k}\Delta)-\cos(2\sqrt{k}\Delta)}\right. \\ &\left. +\frac{2}{3}(p^2-1)\frac{\sinh(\sqrt{k}\Delta)-\sin(\sqrt{k}\Delta)}{\cosh(\sqrt{k}\Delta)+\cos(\sqrt{k}\Delta)}\right]\end{aligned} \tag{4.8}$$

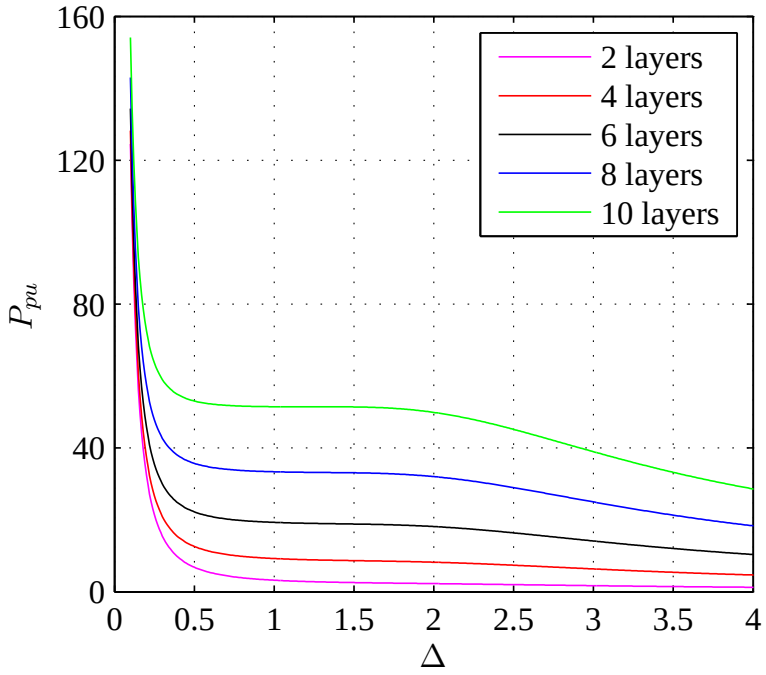

Figure 4.3: Plot of P_{pu} versus Δ for different layers for D=1 and using 1000 harmonics

Fig. 4.2, shows a plot of P_{pu} as the number of harmonics considered is increased. From Fig. 4.2, it can be seen that for a sinusoidal waveform as shown in [3], there exists a valley diameter, hill diameter and a critical diameter whereas for duty-cycle regulated square waveform there is no such minimum. Fig. 4.3 shows a plot of P_{pu} for different layers by considering 1000 harmonics. The reduction in loss is not appreciable from Δ=0.5 to Δ=4. The implication of the results shown in Fig. 4.3 is that, any value of $\Delta > 0.5$ is acceptable if no other factors are considered. However, choosing $\Delta = 0.5$ so as to minimize the amount of copper is not possible in most cases because of thermal considerations. The current density, can be written as,

$$J_{rms} = \frac{I_{rms}}{A} = \frac{I_{rms}}{\frac{\pi d^2}{4}} \tag{4.9}$$

Using, (4.2) and (4.9), yields,

$$\frac{I_{rms}}{J_{rms}} = \frac{2\Delta^2}{\pi^{1.5} f \mu \sigma \eta} \tag{4.10}$$

Simple thermal considerations will yield a maximum allowable J_{rms} for a given core

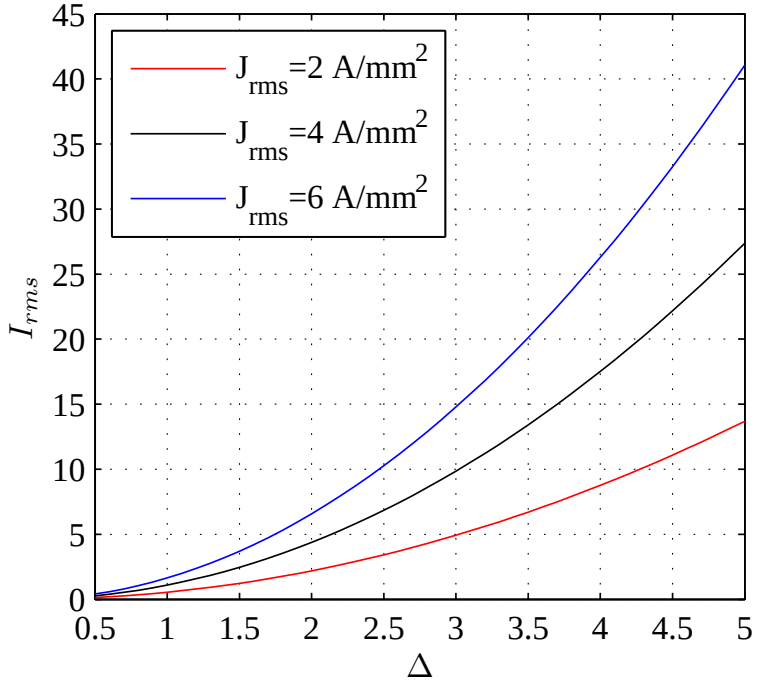

Figure 4.4: Plot of I_{rms} versus Δ for different J_{rms}, for $f = 20kHz$ and $\eta = 0.9$

size. Thus for a given J_{rms} and I_{rms} in (4.10), there will be an associated value of Δ which may be greater than 0.5. Examples of I_{rms} versus Δ are shown in Fig. 4.4 for different values of J_{rms}.

4.1 Approximate power loss expression for different ranges of Δ.

As shown in the previous section, a large number of harmonics have to be considered to compute the AC power loss accurately for a duty-cycle regulated square waveform. As shown in Fig. 4.3 there are three ranges of Δ for which P_{pu} has distinct behavior. This allows for considerable simplification in the estimation of P_{pu}.

4.1.1 Case A : $\Delta < 0.5$

Fig. 4.3, shows a plot of P_{pu} for different layers. From Fig. 4.3, it can be seen that the P_{pu} curve for all layers is very steep for $\Delta < 0.5$. For a fixed current I, as J is increased, Δ will reduce, resulting in less copper. Hence, operating at a value of J allowed by thermal consideration should be appropriate. But in this case, even if the current density value is permissible for $\Delta < 0.5$, the use of that diameter should be avoided to prevent significant losses. The designer can use a bigger diameter to reduce the losses drastically at the cost of increased copper or use either of litz wires or foil conductors. Solving (4.10), by considering that the maximum value of current density is $6A/mm^2$, the limiting value of $\Delta = 0.5$ and $\eta = 0.9$:

$$I_{rms} = 8.213/f \tag{4.11}$$

where, f is in kHz. As an example, for $f = 10kHz$, $I_{rms} > 0.82A$ for a current density of $J_{rms} = 6A/mm^2$. If for a particular application $I_{rms} < 0.82A$, a smaller value of current density should be chosen to avoid the value of $\Delta < 0.5$.

4.1.2 Case B: $0.5 < \Delta < 2.5$

The power loss computation for $0.5 < \Delta < 2.5$ depends on the harmonics and hence is computationally difficult. For $\Delta > 2.5$, both underlined functions in (4.12) become 1 as shown in [31] and hence, the power loss expression can be split as a finite sum and an infinite sum as shown in (4.12) below,

$$\begin{aligned} P_{pu} \;=\; & \sum_{k=1}^{N_\Delta} \frac{\sin^2(\frac{k\pi D}{2})}{k^{\frac{3}{2}}\Delta} \times \left[\underbrace{\frac{\sinh(2\sqrt{k}\Delta) + \sin(2\sqrt{k}\Delta)}{\cosh(2\sqrt{k}\Delta) - \cos(2\sqrt{k}\Delta)}} \right. \\ & \left. + \frac{2}{3}(p^2-1) \underbrace{\frac{\sinh(\sqrt{k}\Delta) - \sin(\sqrt{k}\Delta)}{\cosh(\sqrt{k}\Delta) + \cos(\sqrt{k}\Delta)}} \right] + \left[\left(\frac{2p^2+1}{3\Delta} \right) \sum_{k=N_\Delta+1}^{\infty} \frac{\sin^2\left(\frac{k\pi D}{2}\right)}{k^{\frac{3}{2}}} \right] \end{aligned}$$

where, N_Δ is the harmonic number beyond which the underlined functions become independent of Δ. N_Δ can be found out using, $N_\Delta = \left(\frac{2.5}{\Delta}\right)^2$. The maximum value of N_Δ is 25, corresponding to $\Delta = 0.5$. The infinite sum is a convergent function and hence the power loss can be written as,

$$P_{pu} = \sum_{k=1}^{N_\Delta} \frac{\sin^2(\frac{k\pi D}{2})}{k^{\frac{3}{2}}\Delta} \times \left[\frac{\sinh(2\sqrt{k}\Delta) + \sin(2\sqrt{k}\Delta)}{\cosh(2\sqrt{k}\Delta) - \cos(2\sqrt{k}\Delta)} + \frac{2}{3}(p^2-1)\frac{\sinh(\sqrt{k}\Delta) - \sin(\sqrt{k}\Delta)}{\cosh(\sqrt{k}\Delta) + \cos(\sqrt{k}\Delta)} - \frac{2p^2+1}{3} \right] + \left[\left(\frac{2p^2+1}{3\Delta} \right) \times S \right] \tag{4.12}$$

where,

$$S = \sum_{k=1}^{\infty} \frac{\sin^2\left(\frac{k\pi D}{2}\right)}{k^{\frac{3}{2}}} \tag{4.13}$$

Table 4.1: Infinite series summation value for different D

Duty cycle	$D = 0.25$	$D = 0.5$	$D = 0.6$	$D = 0.75$	$D = 0.8$	$D = 1$
S	1.0785	1.4413	1.5336	1.6293	1.6508	1.6886

The value of the infinite sum depends on duty-ratio D and its value is known as shown in Table 4.1. Hence only a series summation of 25 harmonics is to be considered instead of an infinite series to compute the AC losses.

The example which follows is for the design of a high frequency transformer with turns ratio 1:1 and with the specifications given in Table 4.2.

Table 4.2: Transformer Specifications-I

Parameter	Value
Power	1 kW
Voltage	200 V
Frequency,f	20 kHz
Current Density, J	5 A/mm^2
B_{max}	0.25 T
k_w	0.4

Based on the given specifications as in Table 4.2, using area-product method the core is determined. The chosen core is OP44721EC, ferrite material,and from core datasheet: $c = 24.2$ mm and $D = 7.78$ mm, where c and D are window height and window width

respectively, as shown in Fig. 1. The number of turns, $N = 36$, can be computed as core area is known.

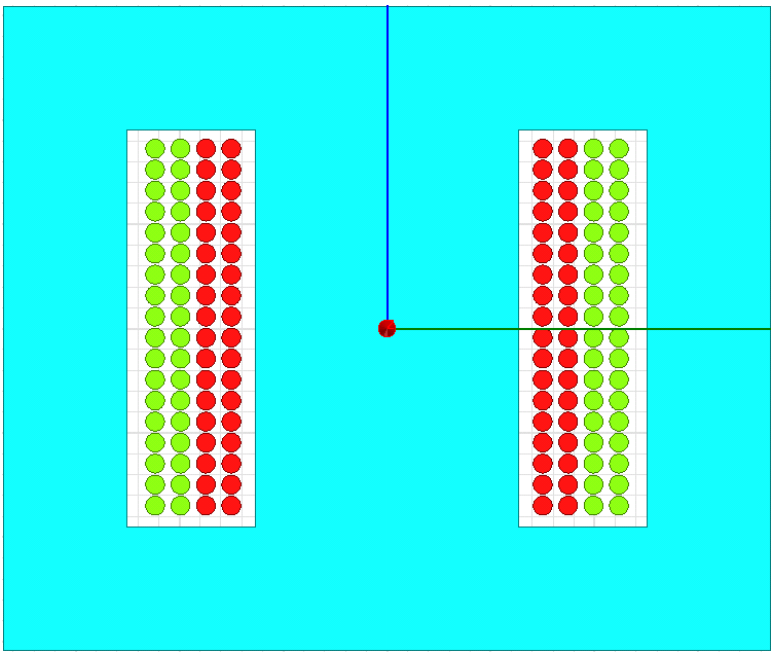

Figure 4.5: 2-D FEM design of Transformer for specifications given in Table 4.2

As the current density value is assumed to be $5A/mm^2$, and the input current, I is known, hence the diameter of the solid-round conductor is fixed.

$$d = \sqrt{\frac{4I}{\pi J}} \tag{4.14}$$

Substituting, J and I in (4.14), $d = 1.1284mm$. The AWG wire 17 of $d = 1.15062mm$ can be chosen. In case of solid-round wire, the height of the window will decide the number of turns per layer, N_l

4.1.3 Case C: $\Delta > 2.5$

As shown in the previous section, the P_{pu} for $\Delta > 2.5$ is simplified as under,

$$P_{pu} = \left[\left(\frac{2p^2 + 1}{3\Delta} \right) \sum_{k=1}^{\infty} \frac{\sin^2\left(\frac{k\pi D}{2}\right)}{k^{\frac{3}{2}}} \right] \tag{4.15}$$

Solving (4.10), by considering that the maximum value of J is $6A/mm^2$, the limiting value of $\Delta = 2.5$ and $\eta = 0.9$:

$$I_{rms} = 205/f \tag{4.16}$$

where, f is in kHz. If the rms current value is greater than the specified value, then $\Delta > 2.5$. As an example, if $I_{rms} > 4.1A$ then $\Delta > 2.5$ for $f = 50kHz$, $J_{rms} = 6A/mm^2$ or less . For $\Delta > 2.5$, the computation of AC losses is extremely simple and the P_{pu}, can be expressed as under,

$$P_{pu} = S \times \left(\frac{2p^2 + 1}{3\Delta}\right) \tag{4.17}$$

S can be obtained from Table 4.1. Fig. 4.8 shows the percentage error in power loss computation by considering 2000 harmonics using (4.8) and, using (4.17) which is independent of harmonics, for a range of Δ from $2.5 - 10$ and for $1 - 10$ layers.

The example which follows is for the design of a high frequency transformer with turns ratio 1:1 and with the specifications given in Table 4.3.

Table 4.3: Transformer Specifications-II

Parameter	Value
Power	5 kW
Voltage	500 V
Frequency,f	50 kHz
Current Density, J	4 A/mm^2
B_{max}	0.25 T
k_w	0.4

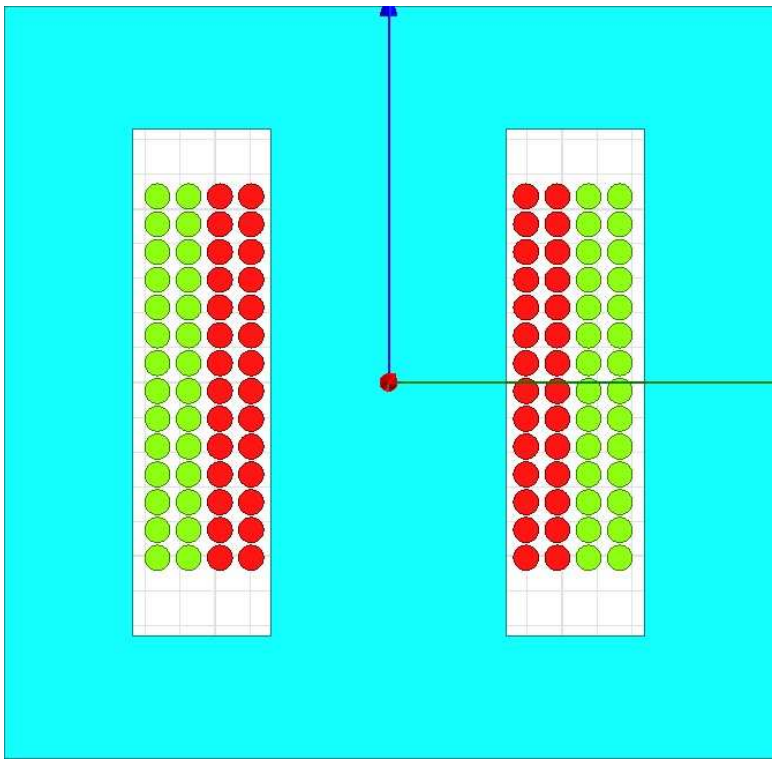

Figure 4.6: 2-D FEM design of Transformer for specifications given in Table 4.3

Based on the given specifications as in Table 4.3, using area-product method the core is determined. The chosen core is OP45528EC, ferrite material,and from core datasheet: c and D can be known, where c and D are window height and window width respectively, as shown in Fig. 1. The number of turns, $N = 28$, can be computed as core area is known. As the current density value is assumed to be $4A/mm^2$, and the input current, I is known, hence the diameter of the solid-round conductor is fixed and can be computed using, (4.14). The value of Δ for the given specification is 4.898. As, $\Delta > 2.5$, hence (4.17) can be used to compute P_{pu} independent of the harmonics. The table in the next section validates the proposed simplified computation with the analytical result and the loss computed using 2-D ANSYS MAXWELL.

4.2 Validation of Results

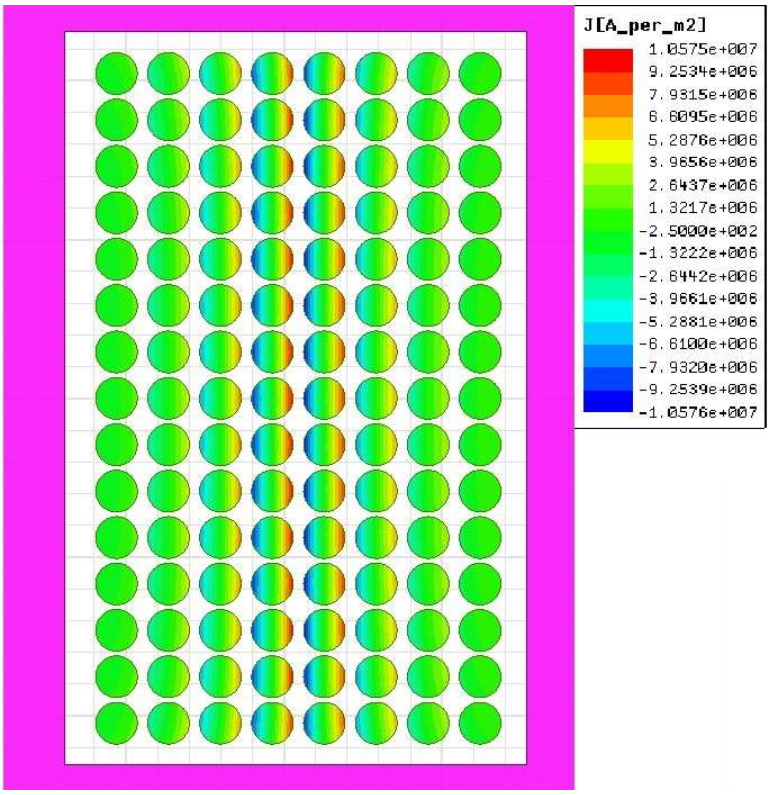

Figure 4.7: Current density distribution by 2-D FEM for a transformer winding with 4 layers

A 2-D Finite element analysis is done to verify the power loss for square waveform of duty ratio $D = 1$, with a rise time of 0.001% using ANSYS MAXWELL 16.0. Simulations are done at $10kHz$, for 2 and 4 layers and for per unit current excitation. Δ depends on the current and the frequency. The validation is done for a range of Δ from $(0.4 - 4.0)$. This allows to validate the results for a wide range of current $(0.05 - 100)$A and frequency $(5 - 100)$kHz and hence a wide range of design specifications. For different design specifications the core sizes will be different. Hence, the window and core sizes are scaled according to Δ to fit the required number of turns/layer. 60 turns for primary and secondary each and 4 values of Δ ranging from $0.4 - 4$ are considered. Fig. 4.7 shows the current density distribution on one side of window of an EE-core for both primary and secondary round conductors containing 4 layers each for a unit excitation of current. $\eta = 0.9$ is assumed for all simulations.

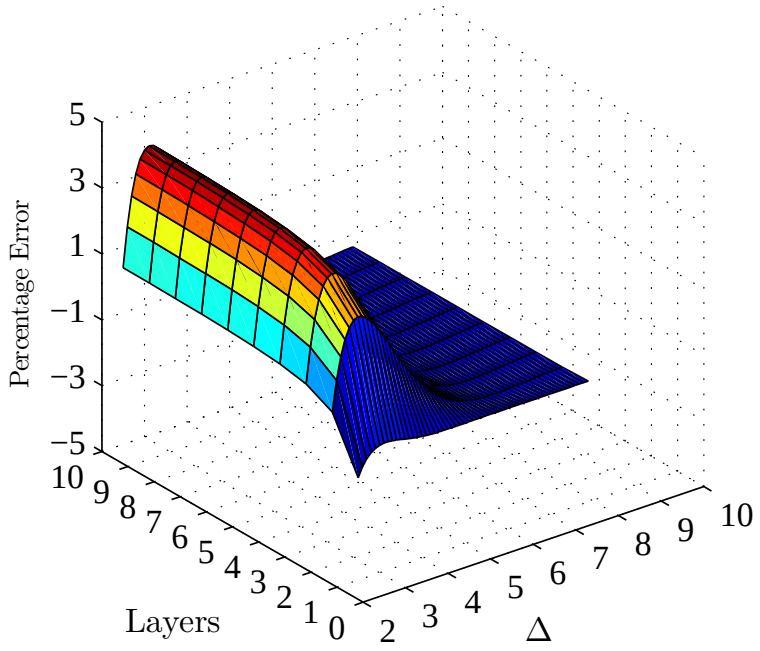

Figure 4.8: Plot of percentage error in P_{pu} for 1-10 layers and $\Delta > 2.5$ by solving (4.8) considering 2000 harmonics and solving (4.17)

P_{pu} is computed analytically using (4.8) considering 5000 harmonics. P_{pu} is also computed using (4.12) considering 25 harmonics for $0.5 < \Delta < 2.5$ and using (4.17) for $\Delta > 2.5$ for 2 and 4 layers. The AC losses are also computed using 2-D FEM and converted into per unit for a square waveform excitation of $1.11072A$ corresponding to $1A$rms fundamental. Fig. 4.9 show a comparison of P_{pu} computed using different methods for 2 and 4 layers respectively. As shown in Fig. 4.9, the approximate expressions are quite close to the analytical values with negligible errors. In the final paper the effect of $\eta < 0.9$ and interleaving between windings will be considered.

Fig. 4.9 validates the proposed power loss formula for a general case. Table 4.4 validates the power loss for 2 specific cases. For the given specifications using area product method the ferrite cores are determined and the number of turns are computed. Assuming η=0.9, the turns are arranged in 2 layers for both specifications. For the first case Δ=4.898 and as Δ >2.5, P_{pu} can be computed using (4.17). For the second case as Δ=1.9488, P_{pu} is computed using (4.12). The final column in Table 4.4 validates the power loss computed using the proposed method (4.12), (4.17) respectively with the

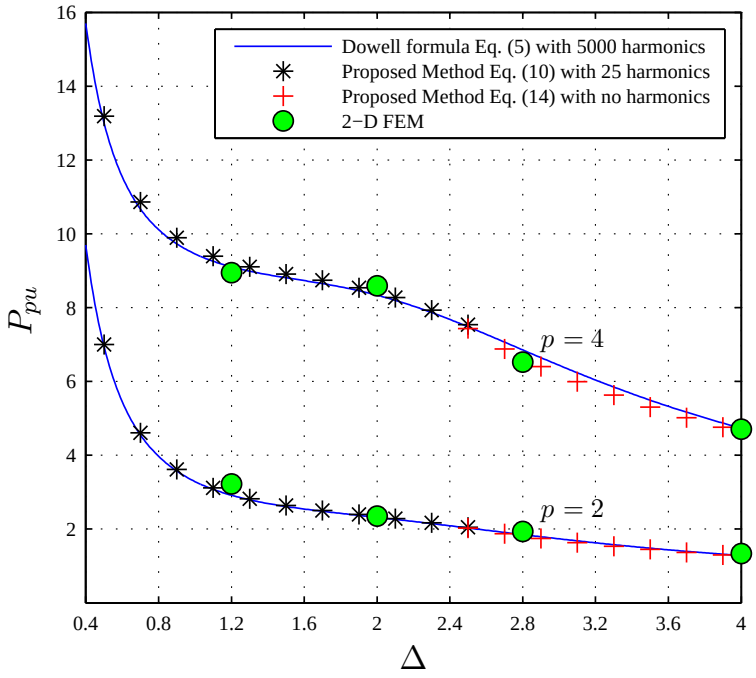

Figure 4.9: Plot of P_{pu} comparison between analytical and 2-D FEM simulation for 2 and 4 layers for $D = 1$ square waveform

conventional method (4.8) and with 2-D FEM. The Mean length turns are calculated as shown in [39].

The next chapter will show a winding design procedure for the foil conductors and the solid-round wire.

Table 4.4: Loss Validation for Specific Transformer Design

Specifications	Core, Layer and Δ	2-D FEM	P_{loss} (W)
V_1=V_2=500 V I_1=I_2=10 A f_s=50kHz J=4; B=0.25 T	OP45528EC Δ= 4.898 p = 2 N = 28 MLT= 0.1376 m	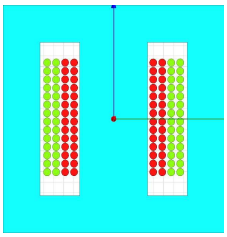	P_{ana}=101.36 W P_{pro}=101.7 W P_{sim}=99.81 W
V_1=V_2=200 V I_1=I_2=5 A f_s = 20kHz J=5; B=0.25 T	OP44721EC Δ= 1.9488 p = 2 N = 36 MLT= 0.125 m	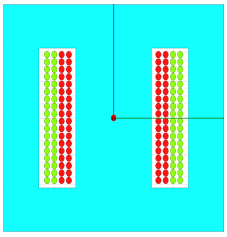	P_{ana}=26.9 W P_{pro}=26.94 W P_{sim}=27.71 W

Chapter 5

High Frequency Transformer Design using Foil and Round Windings

The last few chapters presented approximate expressions to avoid infinite summations for power loss computatuion. But, the ultimate goal of estimating the losses accurately is the winding design. This chapter presents a brief overview of the conventional winding design and demonstrates a different foil winding design to reduce the losses by 30-40 % theoretically.

5.1 Foil winding design based on conventional approach

The ac to dc resistance ratio F_R for foil conductors and sinusoidal current is [6],

$$F_R = \Delta \left[\frac{\sinh(2\Delta) + \sin(2\Delta)}{\cosh(2\Delta) - \cos(2\Delta)} + \frac{2}{3}(p^2 - 1)\frac{\sinh(\Delta) - \sin(\Delta)}{\cosh(\Delta) + \cos(\Delta)} \right] \tag{5.1}$$

where Δ is the ratio of the layer thickness, d and the skin depth, δ at the operating frequency.

$$\Delta = \frac{d}{\delta} \tag{5.2}$$

Fig. 5.1 shows a transformer EE-core with primary and secondary windings.

Fig.5.2 shows a plot of F_R/Δ versus Δ for different layers. The conventional foil winding design procedure is:

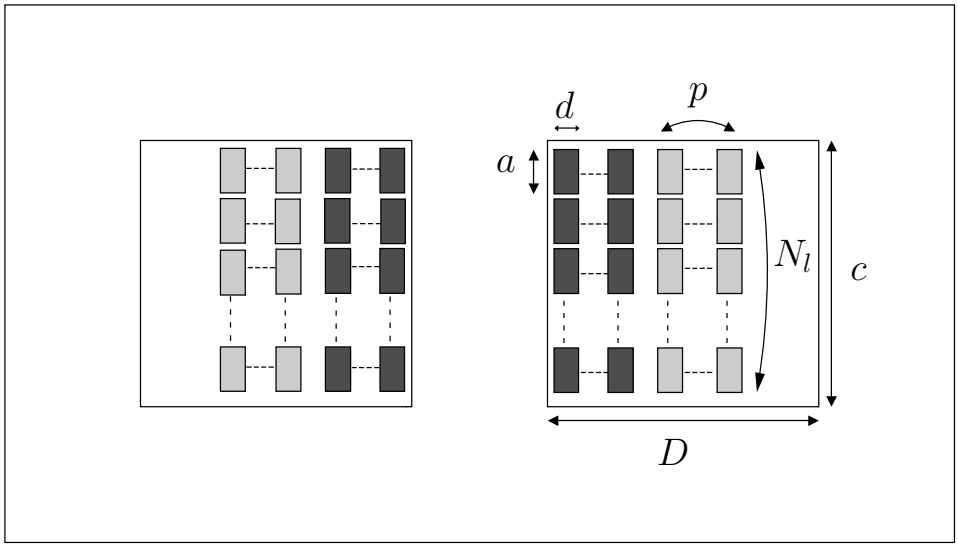

Figure 5.1: Multi-turn Multi-layer foil winding of a transformer.

1 Decide the number of layers, p individually for primary and secondary.

2 Locate Δ_{opt} corresponding to the number of layers chosen from Fig. 5.2.

3 Compute d, the foil conductor thickness from Δ_{opt} as the skin depth is known.

4 Compute a, the width of the conductor from d and J, the current density, using $a = \dfrac{I}{Jd}$.

$$N_l \times a/\eta_1 < c \tag{5.3}$$

5 Check if (5.3) is satisfied, where N_l is the number of turns per layer, η_1 is the layer porosity factor, generally $0.8 - 0.9$ and c is the height of winding.

   (a) If yes, then compute the power loss for the chosen number of layers, p and thickness, d.

   (b) If no, then increase $d > d_{opt}$ to fit in required N_l or change the number of layers, p.

The disadvantage of the above procedure is that it is iterative and there is no fixed way to determine the number of layers to be chosen.

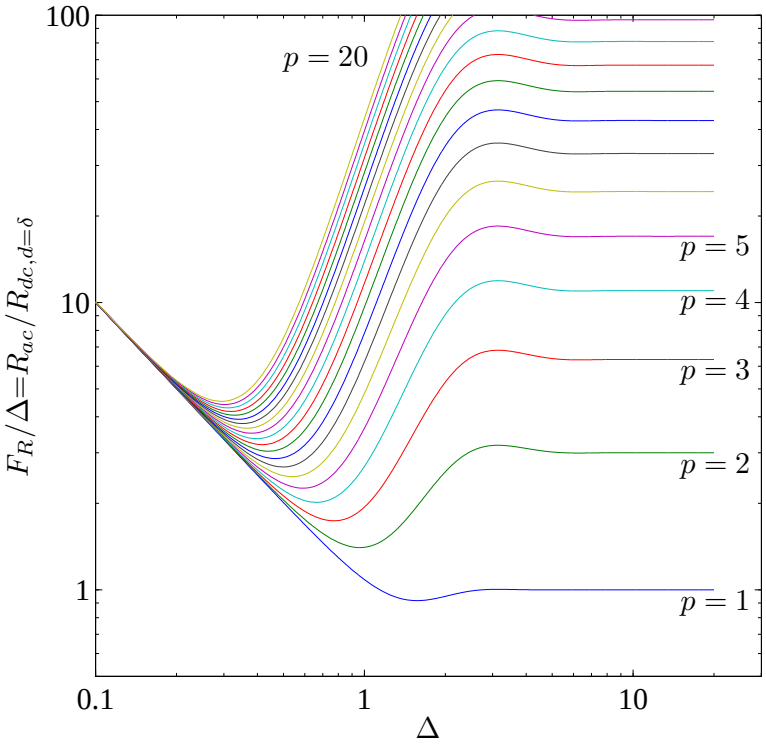

Figure 5.2: Plot of F_R/Δ versus Δ for different layers.

5.2 Foil winding design based on proposed method

The ac losses of a single turn of a transformer is given by (5.4),

$$P_{ac} = I^2 \times R_{dc}|_{d=\delta} \times \frac{F_R}{\Delta} \tag{5.4}$$

where, $R_{dc}|_{d=\delta} = \dfrac{N\rho(MLT)}{a\delta}$. N is the total number of turns, ρ is the resistivity of copper. Since, $a = \dfrac{I}{Jd}$, P_{ac} is,

$$P_{ac} = \frac{IJN(MLT)}{\sigma} \times (F_R) \tag{5.5}$$

Fig. 5.2 shows the plot of F_R/Δ versus Δ for different layers. The Table 5.1 shows in the conventional design, the optimal value of Δ as a function of number of layers. The F_R value varies in a range of 1.36-1.4 for all layers. Hence, if designed at Δ_{opt}, using the conventional method, the foil conductors for any number of layers will give

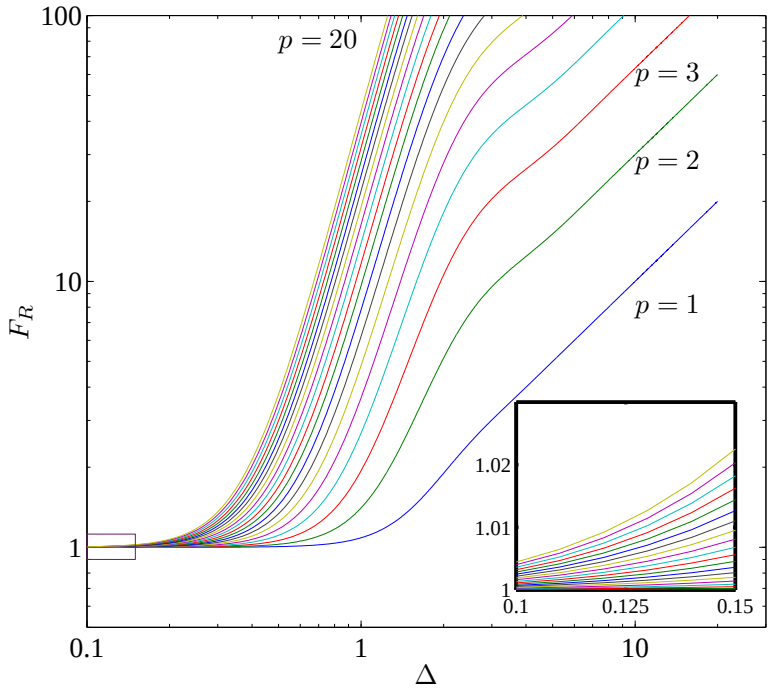

Figure 5.3: Plot of F_R versus Δ for different layers.

approximately the same loss, which obviates the need of interleaving to minimize losses, provided (5.3) is satisfied. If not, then the thickness has to be increased to fit in the required N_l, thereby compensating for increased losses. The reason being, with increasing number of layers the thickness of conductor reduces which increases the width of the foil conductor, and this increase in width counters the increase in losses by the proximity effect.

As seen in Fig. 5.3, by designing the foil conductors in a specific range of Δ, the F_R value can be reduced to close to 1. Fig. 5.4 shows that, using $\Delta_{opt} = 0.43$, which is obtained from Fig. 5.2 for $p = 10$ will give $F_R = 1.379$, but by designing at $\Delta < \Delta_{opt}$ will lead to $F_R < 1.379$ and hence lower losses. By designing at Δ such that F_R is close to 1, the losses can be reduced by 37% compared to the conventional design. Even in the proposed method, by designing the foil conductors such that F_R is close to 1, for all layers, the need of interleaving to minimize the losses can be avoided.

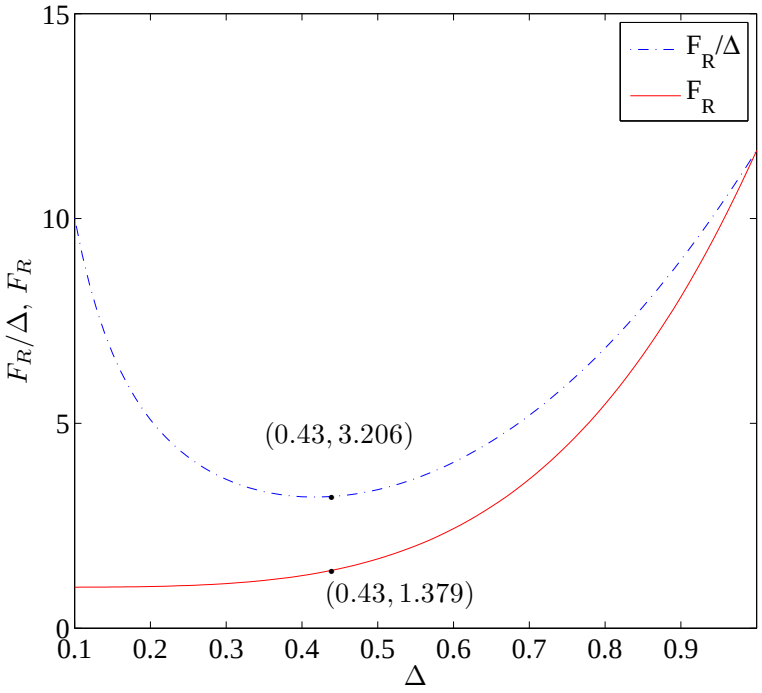

Figure 5.4: Plot of $F_R/\Delta, F_R$ versus Δ for 10 layers.

F_R can be approximated as [31] for $\Delta < 1$,

$$F_R = 1 + \frac{5p^2 - 1}{45}\Delta^4 \tag{5.6}$$

It is not possible to take $F_R = 1$, but it is definitely possible to design with foil thickness, such that F_R is close to 1. For a particular F_R value, Δ as a function of number of layers, can be computed using (5.7). Here, for the designs shown in this thesis, $F_R = 1.05$ is considered. The "proposed method" column in Table 5.1 provides the value of $p\Delta$ product for 1-25 layers for which $F_R = 1.05$.

$$\Delta_{proposed} = \sqrt[0.25]{\frac{45(F_R - 1)}{5p^2 - 1}} \tag{5.7}$$

5.3 Winding Design Procedure for Foil winding and solid-round conductors.

The computation of the minimum winding thickness for a sinusoidal waveform was given by [6] and extended for non-sinusoidal waveform by [31]. But in these methods it is assumed that the number of layers are already known.

The flowchart shown in Fig. 5.5 is a detailed winding design procedure for foil and solid round conductor respectively. For the given specifications using the area product method the core dimensions and number of turns can be known.

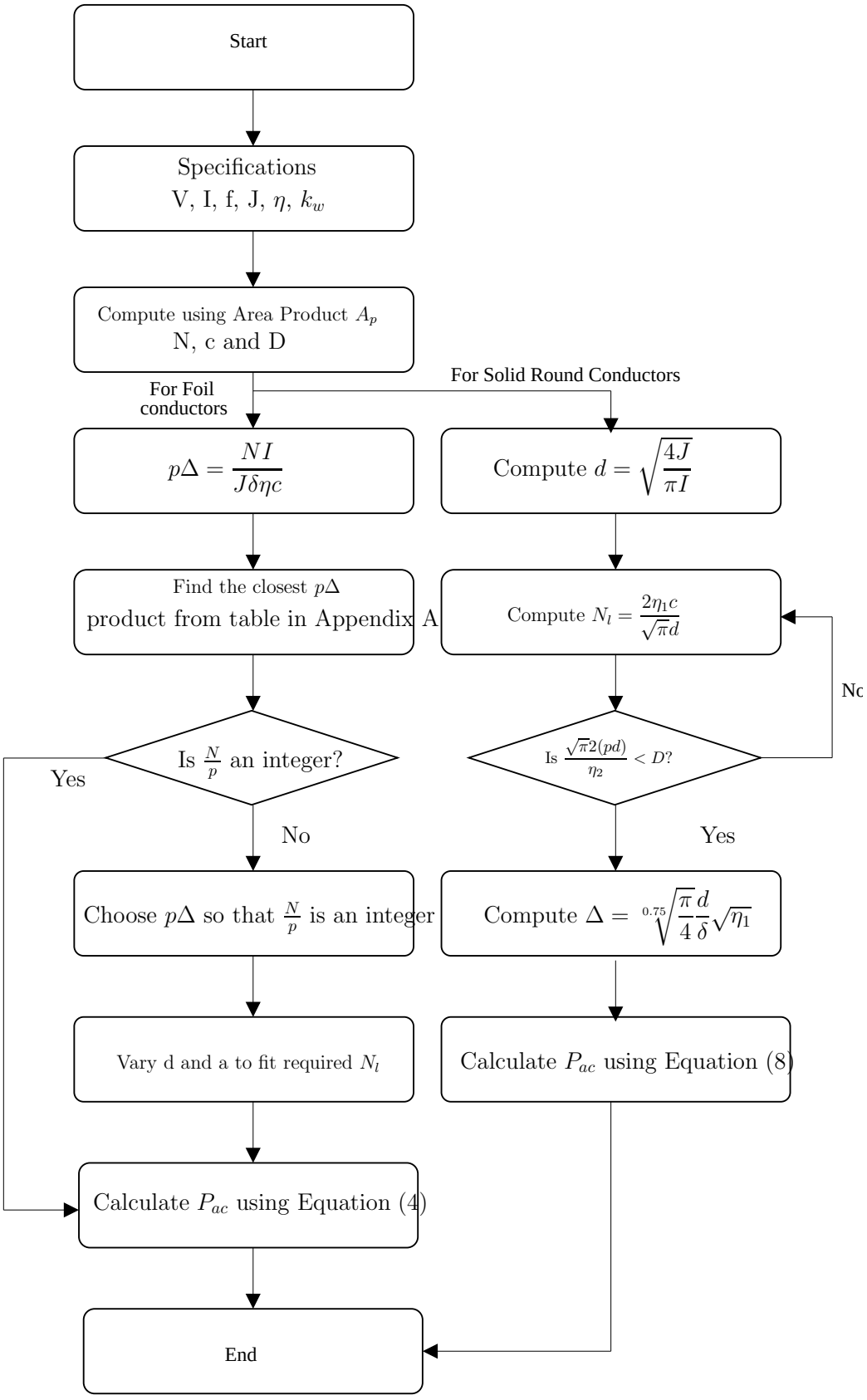

Figure 5.5: Winding design procedure for foil and solid-round conductor.

Now for foil winding, $J = \frac{I}{ad}$, $d = \Delta\delta$, and $\eta_1 = \frac{N_l a}{c}$ where, $N_l = \frac{N}{p}$. Rearranging,

$$p\Delta = \frac{NI}{J\eta_1 \delta c} \tag{5.8}$$

All the quantities on the right hand side of (5.8), are known. From the look up Table 5.1 the number of layers and corresponding Δ can be chosen.

Table 5.1: Parameters to compute $p\Delta$ with the conventional/proposed method .

p	conventional method			proposed method		
-	Δ_{opt}	$p\Delta_{opt}$	F_r	Δ	$p\Delta$	F_r
1	1.58	1.58	1.449	0.88	0.88	1.052
2	0.97	1.94	1.361	0.59	1.18	1.051
3	0.78	2.34	1.356	0.48	1.44	1.052
4	0.67	2.68	1.351	0.41	1.64	1.05
5	0.6	3	1.355	0.37	1.85	1.052
6	0.55	3.3	1.362	0.33	1.98	1.047
7	0.51	3.57	1.365	0.31	2.17	1.05
8	0.48	3.84	1.374	0.29	2.32	1.05
9	0.45	4.05	1.366	0.27	2.43	1.048
10	0.43	4.3	1.376	0.26	2.6	1.05
11	0.41	4.51	1.377	0.25	2.75	1.052
12	0.39	4.68	1.368	0.24	2.88	1.053
13	0.38	4.94	1.387	0.23	2.99	1.052
14	0.36	5.04	1.364	0.22	3.08	1.051
15	0.35	5.25	1.373	0.21	3.15	1.049
16	0.34	5.44	1.377	0.21	3.36	1.055
17	0.33	5.61	1.378	0.2	3.4	1.051
18	0.32	5.76	1.375	0.19	3.42	1.047
19	0.31	5.89	1.368	0.19	3.61	1.052
20	0.3	6	1.359	0.18	3.6	1.046
21	0.3	6.3	1.393	0.18	3.78	1.051
22	0.29	6.38	1.378	0.17	3.74	1.044
23	0.28	6.44	1.361	0.17	3.91	1.049
24	0.28	6.72	1.389	0.17	4.08	1.053
25	0.27	6.75	1.367	0.16	4	1.0455

For solid round wires, the F_R equation as shown in [3] is modified. In case of round

wire, the conductor area depends only on one variable, the conductor diameter. Fig. 5.5 shows a detailed design procedure of solid-round conductor as well.

The power loss formula for solid-round wire is,

$$P_{ac} = I^2\eta_1 \sqrt[1.5]{\frac{\pi}{4}} \times R_{dc}|_{d=\delta} \times \frac{F_R}{\Delta_R^2} \tag{5.9}$$

where, $R_{dc}|_{d=\delta} = \dfrac{N\rho(MLT)}{\dfrac{\pi\delta^2}{4}}$, $\Delta_R = \sqrt[0.75]{\frac{\pi}{4}}\frac{d}{\delta}\sqrt{\eta_1}$ and η_1 is the layer porosity factor as defined in [3].

5.4 Comparison of Foil and Solid-Round Winding

The power loss equation for Foil and round windings is given by (5.5) and (5.9) respectively.Equating the two expression for comparing gives,

$$I\eta_1 \sqrt[1.5]{\frac{\pi}{4}\frac{1}{\frac{\pi\delta^2}{4}}} \times \frac{F_{R_{\Delta_R}}}{\Delta_R^2} = JF_{R_{\Delta_F}} \tag{5.10}$$

Substituting, $\dfrac{I}{J} = A_c = \dfrac{\pi d^2}{4}$, gives,

$$\eta_1 \sqrt[1.5]{\frac{\pi}{4}\frac{d^2}{\delta^2}} \times \frac{F_{R_{\Delta_R}}}{\Delta_R^2} = F_{R_{\Delta_F}} \tag{5.11}$$

Now, $\eta_1 \sqrt[1.5]{\frac{\pi}{4}\frac{d^2}{\delta^2}} = {\Delta_R}^2$, substituting which gives,

$$F_{R_{\Delta_R}} = F_{R_{\Delta_F}} \tag{5.12}$$

which shows that the the round wire should be used if and only if, $F_{R_{\Delta_R}} < F_{R_{\Delta_F}}$.

5.5 Foil winding design using $p\Delta$ product and Validation of Results with 2-D FEM.

The example which follows is for the design of a high frequency transformer with turns ratio 1:1 and with the specifications given in Table 5.2.

Table 5.2: Transformer Specifications

Parameter	Value
Power	1 kW
Voltage	200 V
Frequency,f	20 kHz
Current Density, J	5 A/mm^2
B_{max}	0.3 T
k_w	0.4

Based on the given specifications as in Table 5.2, using area-product method the core is determined. The chosen core is OP44721EC, ferrite material,and from core datasheet: $c = 24.2$ mm and $D = 7.78$ mm, where c and D are window height and window width respectively, as shown in Fig. 1. The number of turns, $N = 36$, can be computed as core area is known.

A 2-D Finite element analysis is done to verify the proposed design methodology using ANSYS MAXWELL 16.0. The winding is excited with a sinusoidal current of $5A$ rms and frequency of 20 kHz. A double EE-core with dimensions of OP44721EC is used. The same core with 6 different winding configurations is analyzed. Four cases are of the foil conductors with/without interleaving for the existing and proposed method and two cases are for round conductors with/without interleaving. The Table 5.3 compares the losses for all cases. A detailed description about the computation of analytical winding loss for all six cases is presented.

5.5.1 Case-A

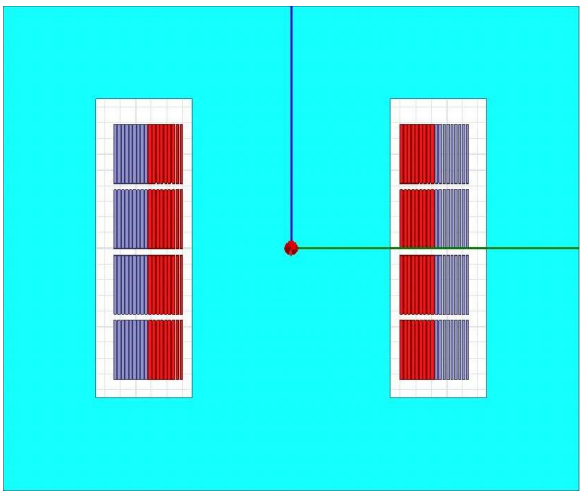

Figure 5.6: Non-interleaved Foil winding with 9 layers designed using existing method.

Fig. 5.6 shows the winding configuration designed using the existing method with 9 layers. As shown in the Fig. 5.6, it is a non-interleaved winding structure with 9 layers of primary having 4 turns/ layer followed by 9 layers of secondary. $\eta = 0.9$ is assumed for all computations. In (5.8) all the parameters on the right hand side are known. Hence $\Delta p = 3.537$. From the "existing method" column in Table 5.2, the number of layers,p, for which Δp is close to 3.537 is $p = 9$. From Fig. 5.2 or the Table 5.2 the value of Δ can be computed, which is 0.45. Now, a, which is the height of foil conductor can be computed from 5.13,

$$a = \frac{I}{J\delta\Delta} \tag{5.13}$$

which gives $a = 4.75mm$. The ac power loss is computed using (5.4) which gives $42.393W/m$. The ac power loss can also be computed using (5.5) which gives the same result and it shows that $F_R = 1.366$. Even if, $p = 18$ would have been chosen then still the losses would have been around the same value as in that case the width of the conductor would be increased such that the F_R is around $1.36 - 1.4$

5.5.2 Case-B

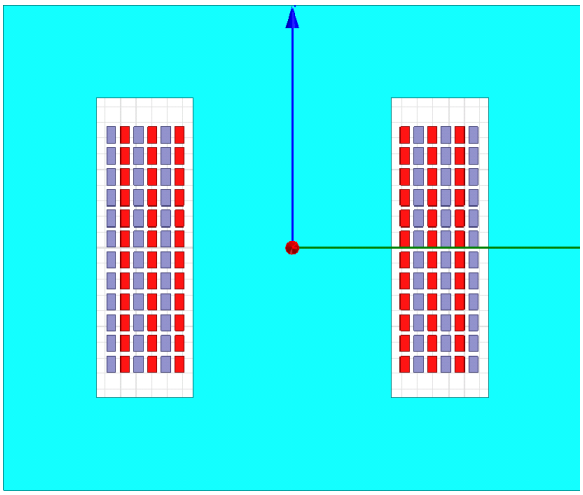

Figure 5.7: Interleaved Foil winding with 1 layer designed using existing method.

If interleaving of primary and secondary winding is considered then the best possible way is to have 1-layer of primary and 1-layer of secondary. Fig. 5.7 shows the above described winding configuration. For such a configuration, $\Delta p = 1.58$ using Dowell's curve shown in Fig. 5.2. Using, the above data, number of turns in 1-layer of primary winding can be selected using,

$$N = \frac{\Delta p J \delta \eta_1 c}{I} \tag{5.14}$$

which gives $N = 14.29$. $N_l = 12$ is chosen in order to realize the 36 turns which are already fixed. The winding arrangement will be 3 sets of 12 turns of primary followed by 12 turns of secondary. In this case, $a = 1.35mm$ using (5.13) and the ac power loss is $44.96W/m$.

The analytical ac loss is around the same as that of the case with non-interleaved winding. This is because, the width of the conductor is less in case of single layer as compared to the non-interleaved case. If the design is such that the thickness is the same and the number of layers are increased then the losses for single layer would be less. But in general, with the increase in the number of layers, the thickness is reduced as seen by "existing method" column in Table 5.2, as proposed in previous literature, hence the losses are almost the same.

5.5.3 Case-C

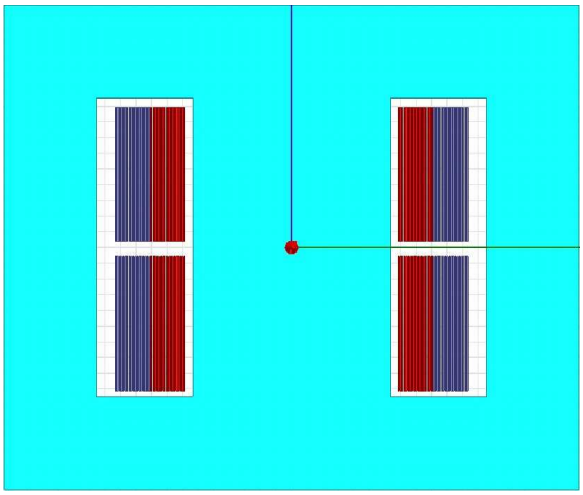

Figure 5.8: Non-interleaved Foil winding with 18 layers designed using proposed method.

Fig. 5.8 shows the winding configuration designed using the proposed method with 18 layers. As shown in the Fig. 5.8, it is a non-interleaved winding structure with 18 layers of primary having 2 turns/ layer followed by 18 layers of secondary. If instead of using Dowell's curve, the curve as shown in Fig. 5.3 is used, then the Δ can be selected such that $F_R = 1$, provided the computed width of the conductor satisfies (5.3). Here, in this analysis Δ is chosen such that $F_R = 1.05$.

In the example considered, the $\Delta p = 3.537$. From the "proposed method" column in Table 5.2, the number of layers, p, for which Δp is close to 3.537 is $p = 18$. From Fig. 5.2 or the Table 5.2 the value of Δ can be computed, which is 0.19. Now, a, which is the height of foil conductor can be computed from 5.13, which gives $a = 11.2629mm$. This value of a will not satisfy (5.3). Hence, Δ, should be chosen so as to allow 2 turns/layer. Considering, $\Delta = 0.1965$ will allow 2 turns/layers but, $F_R = 1.0536 > 1.05$ but still less than 1.37. In this case, $a = 10.89mm$. The ac power loss is computed using (5.4) which gives $32.698W/m$. The ac power loss can also be computed using (5.5) which gives the same result and it shows that $F_R = 1.0536$.

5.5.4 Case-D

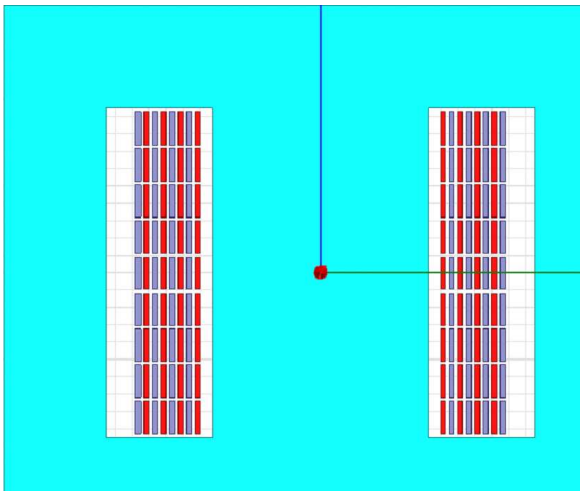

Figure 5.9: Interleaved Foil winding with 1 layer designed using proposed method.

Fig. 5.9 shows the winding configuration designed using the proposed method with interleaving of primary and secondary winding. As shown in the Fig. 5.9, it is an inter-leaved winding structure with 4 sets of 9 turns of primary followed by 9 turns of secondary. For such a configuration, number of turns in 1-layer of primary winding can be selected from the "proposed method" column in Table 5.2 using $\Delta p = 0.88$ in (5.14) .

Using, the above data, number of turns in 1-layer of primary winding can be selected from, (5.14) which gives $N = 9$. Using, $\Delta = 0.88$, the $\Delta F_R = 1.05$. In this case, the ac power loss is $32.586 W/m$.

5.5.5 Case-E

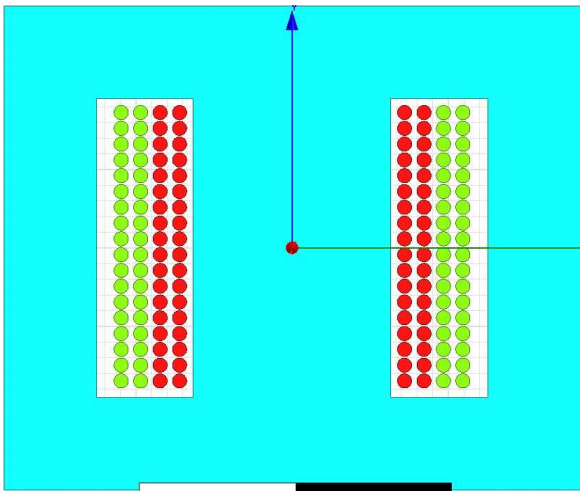

Figure 5.10: Non-interleaved Round conductors with 2 layers.

Fig. 5.10 shows the winding configuration designed using the round conductors without interleaving the primary and secondary winding. The flowchart as shown in Fig. 5.5 is followed for round conductors. As the given case is a non-interleaved structure, both layers of primary are wound together. As Δ is a constant in case of round conductors, hence the losses will increase due to proximity effects.

5.5.6 Case-F

Fig. 5.11 shows the winding configuration designed using the round conductors by interleaving the primary and secondary winding. As a result of interwinding, the losses are reduced in comparison to the non-interleaved case.

The analytical and simulated losses are computed per unit length. The average mean length of turns can be chosen as 0.125 m according to [45]. The results match closely with the analytical calculation for foil conductors but are different for round winding due to 2-D effects.

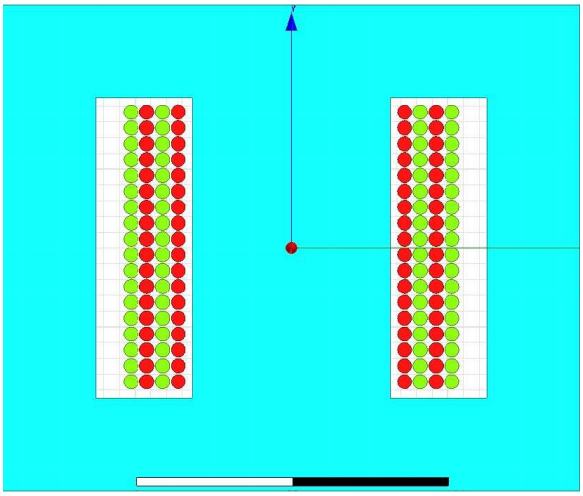

Figure 5.11: Interleaved Round conductors with 1 layer.

Table 5.3: Validation of results with 2-D FEM.

Case	$p\Delta$	p	N_l	Δ	a	Analytical P	Simulated P	F_R
Existing Method Non-interleaving	3.537	9	4	0.45	4.75 mm	5.3 W	5.34 W	1.366
Existing Method Interleaving	1.58	1	12	1.58	1.35 mm	5.62 W	4.85 W	1.449
Proposed Method Non-Interleaving	3.537	18	2	0.1965	10.89 mm	4.087 W	4.23 W	1.0536
Proposed Method Interleaving	0.9	1	9	0.9	2.378 mm	4.073 W	4.044 W	1.058
Round winding Non-Interleaving	-	2	18	1.9488	-	18.22 W	15.93 W	-
Round winding Interleaving	-	1	18	1.9488	-	6.86 W	6.3625 W	-

Chapter 6

Conclusion and Future Work

The copper loss in a multi-layer transformer foil/round winding for a particular duty-cycle modulated current waveform at a given frequency depends on the number of layers and the thickness of each layer. It has been shown that Fourier series method requires consideration of a large number of harmonics leading to computational difficulty of power loss. In contrast, an approximate closed form expression for power loss has been derived that does not involve any series summation of harmonics for foil conductors. In case of solid-round wire there is no optimum diameter where the AC losses are minimum. The whole range of normalized diameter is split into three cases and simplified power loss expressions have been provided for them. The accuracy of the expression is verified using numerical computation as well as with 2-D FEM. A designer can simply use these formulas instead of writing complex computationally demanding MATLAB codes to obtain optimal thickness and estimate the copper loss.

The thesis also demonstrates the winding design with foil/round conductors for sinusoidal excitation. It has been shown that, if the winding is designed at a thickness lower than the "optimal" thickness, as given in literature, for a specific layer then the losses can be minimized. Theoretically, power loss can be reduced around 36-40%, depending on the number of layers. The ac-to-dc resistance ratio close to 1 can be achieved using foil conductors provided the winding can fit inside the window. Hence, it can replace the expensive litz wires which also have low window utilization factor. The thesis also demonstrates that a proper design can help to avoid interleaving in case of foil conductors for minimizing winding loss. The paper also presents a comparison between

foil and round conductors in terms of winding losses. Six different winding configurations with/without interleaving, foil/round conductors for the same specification and on the same EE-core are analyzed using 2-D FEM simulations. For all six cases losses are computed and compared with analytical results. The results show that interleaving of winding is a must in case of solid- round conductors whereas interleaving can be avoided in case of foil winding if designed properly.

6.1 Future Work

- Design a prototype to validate the analytical/2-D FEM losses in foil/solid-round wire conductors for a duty-cycle regulated square waveform.
- Design six different winding configuration of the same specification and validate the analytical/FEM results using hardware.
- The winding design procedure has been shown for a sinusoidal excitation but can be easily extended to non-sinusoidal waveform by incorporating the series summation and the range of thickness for which the ac-to-dc resistance is 1 can be derived.
- The winding design procedure can be modified in a manner to obtain a design that gives minimum leakage inductance.
- The given winding design procedure is for power levels for which core is available. In the future, it can be extended for a winding design for higher power level.

References

[1] R. Petkov. Optimum design of a high-power, high-frequency transformer. *Power Electronics, IEEE Transactions on*, 11(1):33–42, 1996.

[2] W.-J. Gu and R. Liu. A study of volume and weight vs. frequency for high-frequency transformers. In *Power Electronics Specialists Conference, 1993. PESC '93 Record., 24th Annual IEEE*, pages 1123–1129, 1993.

[3] R.P. Wojda and M.K. Kazimierczuk. Analytical optimization of solid x2013;round-wire windings. *Industrial Electronics, IEEE Transactions on*, 60(3):1033–1041, 2013.

[4] E. BENNETT and S. C. LARSEN. Effective resistance to alternating currents of multilayer windings. *Trans. Amer. Inst. Elect. Engrs.*, 59:1010, 1940.

[5] T.H. LONG. Eddy-current resistance of multilayer coils. *ibid.*, 64:71, 1945.

[6] P.L. Dowell. Effects of eddy currents in transformer windings. *Electrical Engineers, Proceedings of the Institution of*, 113(8):1387 –1394, august 1966.

[7] F. Robert, P. Mathys, and J.-P. Schauwers. Ohmic losses calculation in smps transformers: numerical study of dowell's approach accuracy. *Magnetics, IEEE Transactions on*, 34(4):1255–1257, 1998.

[8] F. Robert, P. Mathys, and J.-P. Schauwers. A closed-form formula for 2-d ohmic losses calculation in smps transformer foils. *Power Electronics, IEEE Transactions on*, 16(3):437–444, 2001.

[9] D.R. Zimmanck and C.R. Sullivan. Efficient calculation of winding-loss resistance matrices for magnetic components. In *Control and Modeling for Power Electronics (COMPEL), 2010 IEEE 12th Workshop on*, pages 1–5, 2010.

[10] C.R. Sullivan. Computationally efficient winding loss calculation with multiple windings, arbitrary waveforms, and two-dimensional or three-dimensional field geometry. *Power Electronics, IEEE Transactions on*, 16(1):142–150, 2001.

[11] M. Vitelli. Numerical evaluation of 2-d proximity effect conductor losses. *Power Delivery, IEEE Transactions on*, 19(3):1291–1298, 2004.

[12] W.A. Roshen. High-frequency fringing fields loss in thick rectangular and round wire windings. *Magnetics, IEEE Transactions on*, 44(10):2396–2401, 2008.

[13] F. Robert, P. Mathys, B. Velaerts, and J.-P. Schauwers. Two-dimensional analysis of the edge effect field and losses in high-frequency transformer foils. *Magnetics, IEEE Transactions on*, 41(8):2377–2383, 2005.

[14] A.M. Urling, V.A. Niemela, G.R. Skutt, and T.G. Wilson. Characterizing high-frequency effects in transformer windings-a guide to several significant articles. In *Applied Power Electronics Conference and Exposition, 1989. APEC' 89. Conference Proceedings 1989., Fourth Annual IEEE*, pages 373–385, 1989.

[15] J.-P. Vandelac and P.D. Ziogas. A novel approach for minimizing high-frequency transformer copper losses. *Power Electronics, IEEE Transactions on*, 3(3):266–277, 1988.

[16] V.A. Niemela, G.R. Skutt, A.M. Urling, Y.-N. Chang, T.G. Wilson, Jr. Owen, H.A., and R.C. Wong. Calculating the short-circuit impedances of a multiwinding transformer from its geometry. In *Power Electronics Specialists Conference, 1989. PESC '89 Record., 20th Annual IEEE*, pages 607–617 vol.2, 1989.

[17] F. Robert, P. Mathys, and J.-P. Schauwers. The layer copper factor, although widely used and useful, has no theoretical base [smps transformers]. In *Power Electronics Specialists Conference, 2000. PESC 00. 2000 IEEE 31st Annual*, volume 3, pages 1633–1638 vol.3, 2000.

[18] J.-P. Vandelac and P.D. Ziogas. A novel approach for minimizing high-frequency transformer copper losses. *Power Electronics, IEEE Transactions on*, 3(3):266–277, 1988.

[19] M.P. Perry. Multiple layer series connected winding design for minimum losses. *Power Apparatus and Systems, IEEE Transactions on*, PAS-98(1):116–123, 1979.

[20] J.A. Ferreira. Aring;nalytical computation of ac resistance of round and rectangular litz wire windings. *Electric Power Applications, IEE Proceedings B*, 139(1):21–25, 1992.

[21] J.A. Ferreira. Improved analytical modeling of conductive losses in magnetic components. *Power Electronics, IEEE Transactions on*, 9(1):127–131, 1994.

[22] Xi Nan and C.R. Sullivan. Simplified high-accuracy calculation of eddy-current loss in round-wire windings. In *Power Electronics Specialists Conference, 2004. PESC 04. 2004 IEEE 35th Annual*, volume 2, pages 873–879 Vol.2, 2004.

[23] Xi Nan and C.R. Sullivan. An improved calculation of proximity-effect loss in high-frequency windings of round conductors. In *Power Electronics Specialist Conference, 2003. PESC '03. 2003 IEEE 34th Annual*, volume 2, pages 853–860 vol.2, 2003.

[24] F. Robert. A theoretical discussion about the layer copper factor used in winding losses calculation. *Magnetics, IEEE Transactions on*, 38(5):3177–3179, 2002.

[25] E. C. Snelling. *Soft Ferrites: Properties and Applications*. U.K.: Illife Books, 1969.

[26] Marian K Kazimierczuk. *High-frequency magnetic components*. Wiley. com, 2009.

[27] Chenhao Nan and Raja Ayyanar. Dual active bridge converter with pwm control for solid state transformer application. In *Energy Conversion Congress and Exposition (ECCE), 2013 IEEE*, pages 4747–4753, 2013.

[28] K. D. Hoang and J. Wang. Design optimization of high frequency transformer for dual active bridge dc-dc converter. In *Electrical Machines (ICEM), 2012 XXth International Conference on*, pages 2311–2317, 2012.

[29] PS Venkatraman. Winding eddy current losses in switch mode power transformers due to rectangular wave currents. In *Proceedings of Powercon*, volume 11, pages 1–11, 1984.

[30] S. Crepaz. Eddy-current losses in rectifier transformers. *Power Apparatus and Systems, IEEE Transactions on*, PAS-89(7):1651 –1656, sept. 1970.

[31] W.G. Hurley, E. Gath, and J.G. Breslin. Optimizing the ac resistance of multilayer transformer windings with arbitrary current waveforms. *Power Electronics, IEEE Transactions on*, 15(2):369 –376, mar 2000.

[32] M.E. Dale and C.R. Sullivan. General comparison of power loss in single-layer and multi-layer windings. In *Power Electronics Specialists Conference, 2005. PESC '05. IEEE 36th*, pages 582 –589, june 2005.

[33] R.P. Wojda and M.K. Kazimierczuk. Analytical optimisation of solid-round-wire windings conducting dc and ac non-sinusoidal periodic currents. *Power Electronics, IET*, 6(7):1462–1474, 2013.

[34] K. Iyer, K. Basu, W. Robbins, and N. Mohan. Determination of the optimal thickness for a multi-layer transformer winding. In *Energy Conversion Congress and Exposition (ECCE), 2013 IEEE*, 2013.

[35] A.I. Maswood and Lim Keng Song. Design aspects of planar and conventional smps transformer: a cost benefit analysis. *Industrial Electronics, IEEE Transactions on*, 50(3):571–577, 2003.

[36] A. Nysveen and M. Hernes. Minimum loss design of a 100 khz inductor with foil windings. In *Power Electronics and Applications, 1993., Fifth European Conference on*, pages 106–111 vol.3, 1993.

[37] J. Schutz, J. Roudet, and A. Schellmanns. Modeling litz wire windings. In *Industry Applications Conference, 1997. Thirty-Second IAS Annual Meeting, IAS '97., Conference Record of the 1997 IEEE*, volume 2, pages 1190–1195 vol.2, 1997.

[38] A. M. Tuckey and D.J. Patterson. A minimum loss inductor design for an actively clamped resonant dc link inverter. In *Industry Applications Conference, 2000. Conference Record of the 2000 IEEE*, volume 5, pages 3119–3126 vol.5, 2000.

[39] Ned Mohan and Tore M Undeland. *Power electronics: converters, applications, and design*. Wiley. com, 2007.

[40] W.G. Hurley, W.H. Wolfle, and J.G. Breslin. Optimized transformer design: inclusive of high-frequency effects. *Power Electronics, IEEE Transactions on*, 13(4):651–659, 1998.

[41] Charles R Sullivan. Optimal choice for number of strands in a litz-wire transformer winding. In *Power Electronics Specialists Conference, 1997. PESC'97 Record., 28th Annual IEEE*, volume 1, pages 28–35. IEEE, 1997.

[42] C.R. Sullivan. Cost-constrained selection of strand diameter and number in a litz-wire transformer winding. *Power Electronics, IEEE Transactions on*, 16(2):281–288, 2001.

[43] M.H. Kheraluwala, D.W. Novotny, and D.M. Divan. Design considerations for high power high frequency transformers. In *Power Electronics Specialists Conference, 1990. PESC '90 Record., 21st Annual IEEE*, pages 734–742, 1990.

[44] J.G. Breslin and W.G. Hurley. Derivation of optimum winding thickness for duty cycle modulated current waveshapes. In *Power Electronics Specialists Conference, 1997. PESC '97 Record., 28th Annual IEEE*, volume 1, pages 655 –661 vol.1, jun 1997.

[45] Ned Mohan, Tore M Undeland, and William P Robbins. Power electronics: converters, applications, and design. 1989.

Appendix A

Winding Power Loss in Rectangular Co-ordinate System

Maxwell's equations in a linear homogeneous isotropic medium for a magnetoquasistatic system, takes the following form:

$$\nabla \times \overrightarrow{E} = -\mu_0 \frac{\partial \overrightarrow{H}}{\partial t} \tag{A.1}$$

$$\nabla \times \overrightarrow{H} = \sigma \overrightarrow{E} + \mu_0 \epsilon_0 \frac{\partial \overrightarrow{E}}{\partial t} \tag{A.2}$$

For a sinusoidal current, $I = I_o \sin(\omega t)$, and assuming that the conductor is infinitely long so that the magnetic field, B is only in the y-direction and the electric field E is only in the z-direction, the Maxwell's equations reduce to:

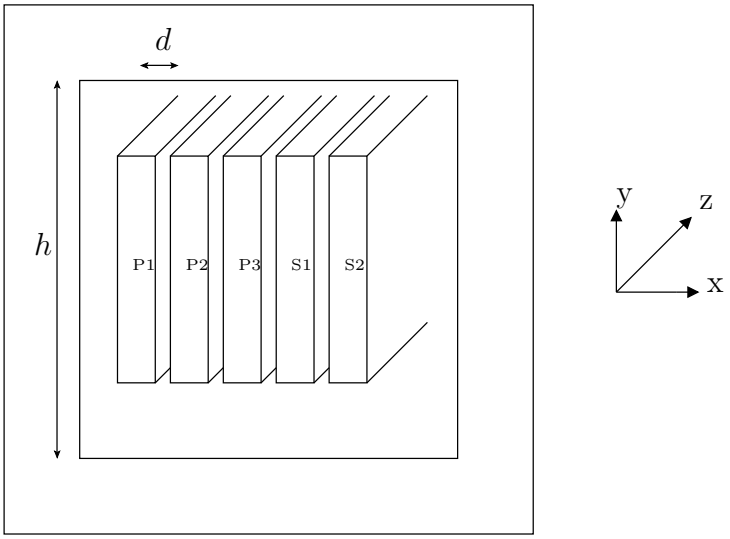

Figure A.1: Primary and secondary Transformer windings

$$\nabla \times \overrightarrow{E} = -j\omega\mu_0 \overrightarrow{H} \tag{A.3}$$

$$\nabla \times (\nabla \times \overrightarrow{H}) = \sigma(\nabla \times \overrightarrow{E}) = -j\omega\sigma\mu_0 \overrightarrow{H} \tag{A.4}$$

$$\nabla^2 \overrightarrow{H} = j\omega\sigma\mu_0 \overrightarrow{H} \tag{A.5}$$

$$\hat{k}\sigma E_z = \begin{vmatrix} \hat{i} & \hat{j} & \hat{k} \\ \frac{\partial}{\partial x} & \frac{\partial}{\partial y} & \frac{\partial}{\partial z} \\ 0 & H_y & 0 \end{vmatrix}.$$

$$\hat{k}\sigma E_z = -\frac{\partial H_y}{\partial z}\hat{i} + \frac{\partial H_y}{\partial x}\hat{k} \tag{A.6}$$

$$\sigma E_z = \frac{\partial H_y}{\partial x} \tag{A.7}$$

$$\nabla \times \overrightarrow{E} = -\hat{j}j\omega\mu_0 H_y = \begin{vmatrix} \hat{i} & \hat{j} & \hat{k} \\ \frac{\partial}{\partial x} & \frac{\partial}{\partial y} & \frac{\partial}{\partial z} \\ 0 & 0 & E_z \end{vmatrix}.$$

$$\frac{\partial E_z}{\partial x} = j\omega\mu_0 H_y \tag{A.8}$$

$$\frac{\partial^2 H_y}{\partial x^2} = j\omega\mu_0\sigma H_y \tag{A.9}$$

$$H_y = {H_y}^+ e^{-mx} + {H_y}^- e^{mx} \tag{A.10}$$

where, $m^2 = j\omega\mu_0\sigma$

$$H(x_{ni}) = (n-1)H_0 \tag{A.11}$$

$$H(x_{no}) = nH_0 \tag{A.12}$$

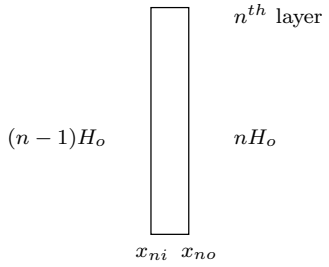

Figure A.2: Isolated single foil conductor

Let, $x_{ni} = a$ and $x_{no} = b$. Applying, inner and outer boundary conditions on layer, n,

$$H_y(a) = {H_y}^+ e^{-ma} + {H_y}^- e^{ma} = (n-1)H_0 \tag{A.13}$$

$$H_y(b) = {H_y}^+ e^{-mb} + {H_y}^- e^{mb} = nH_0 \tag{A.14}$$

Solving,

$${H_y}^+ = \frac{nH_0(e^{mb} - e^{ma}) - H_0 e^{mb}}{e^{m(b-a)} - e^{-m(b-a)}} \tag{A.15}$$

$${H_y}^- = \frac{nH_0(e^{-ma} - e^{-mb}) + H_0 e^{-mb}}{e^{m(b-a)} - e^{-m(b-a)}} \tag{A.16}$$

Using, $\sigma E_z = \frac{\partial H_y}{\partial x}$,

$$E_z(x) = \frac{m}{\sigma}\left[{H_y}^- e^{mx} - {H_y}^+ e^{-mx}]\right] \tag{A.17}$$

Now, the power per unit length on the inside and the outside of the layer is,

$$P_a = E(a)H(a)h \tag{A.18}$$

$$P_b = E(b)H(b)h \tag{A.19}$$

respectively,where, h is the width of the conductor, which is considered as a constant. Substituting values of $E(a), H(a), E(b), H(b)$ and solving we get,

$$P_a = \frac{mw(n-1)H_0}{\sigma e^{m(b-a)} - e^{-m(b-a)}}\left[2nH_0 + H_0 e^{-m(b-a)} + e^{m(b-a)} - nH_0 e^{-m(b-a)} - e^{m(b-a)}\right] \tag{A.20}$$

$$P_b = \frac{mhnH_0}{\sigma e^{m(b-a)} - e^{-m(b-a)}}\left[2H_0 - 2nH_0 + nH_0 e^{-m(b-a)} + e^{m(b-a)}\right] \tag{A.21}$$

Solving further,

$$P_a - P_b = \frac{mhH_0^2}{\sigma}\left[\coth(md) + 2n(n-1)\tanh(\frac{md}{2})\right] \tag{A.22}$$

Substituting, $H_0 = \frac{N_l I}{h}$, where N_l is the number of turns per layer. Solving for p layers, gives,

$$P = 2I^2\frac{\rho(MLT)N^2}{h\delta p\eta}\left[\frac{\sinh(2\Delta) + \sin(2\Delta)}{\cosh(2\Delta) - \cos(2\Delta)} + \frac{2}{3}(p^2-1)\frac{\sinh(\Delta) - \sin(\Delta)}{\cosh(\Delta) + \cos(\Delta)}\right] \tag{A.23}$$